BioMed

MDPI

Article

Single-Eye Porcine Retinal Pigment Epithelium Cell Cultures—A Validated and Reproducible Protocol

Philipp Dörschmann *, Justine Wilke, Nina Tietze, Johann Roider and Alexa Klettner

Department of Ophthalmology, University Medical Center, Kiel University, Arnold-Heller-Str. 3, Haus B2, 24105 Kiel, Germany; johann.roider@uksh.de (J.R.); alexa.klettner@uksh.de (A.K.)
* Correspondence: philipp.doerschmann@uksh.de; Tel.: +49-500-13712

Abstract: Background: Age-related macular degeneration (AMD) is the leading cause of severe vision loss in industrialized nations. AMD models based on standardized optimized cell culture models are warranted. The aim of this study is to implement a standard operation protocol for the preparation of porcine retinal pigment epithelium (RPE) from pig eyes with cells from one eye designated for one culture, generating a genetic homology within one culture and genetic heterogeneity between cultures, thereby implementing a relevant in vitro model for AMD investigations. In addition, the use of pigs' eyes from slaughterhouse waste material is an active measure to reduce animal experimentation in ophthalmological research. **Methods**: Primary porcine RPE cells were prepared, and cells from one eye were seeded into one well of a twelve-well polystyrene plate. They were cultured for 7, 14, and 28 days. Different post-mortem times (2, 4, and 6 h), coatings (collagen I, IV, Poly-D-Lysine, fibronectin, and laminin), and serum content of media (1%, 5%, and 10%) were tested. The success rate for confluence and survival was determined. At the different time points, cell number (trypan blue exclusion assay), confluence and morphology (microscope imaging), VEGF content of supernatants, and gene and protein expression, as well as tight junctions (fluorescence imaging), were examined. In addition, a baseline for RPE morphometry using CellProfiler software was established. **Results**: A post-mortem time of 4 to 5 h is most suitable. A coating with Poly-D-Lysine is recommended due to high success rates, the fastest confluence, the highest expression of RPE65, and suitable morphologic properties. The results for confluence, protein expression, and morphology showed that a reduction of 10% to 5% FBS is acceptable. **Conclusion**: A basic best practice protocol for the preparation of porcine single-eye cultures with optimized parameters was established and is provided.

Keywords: morphology; cell number; 3R principle; best practice protocol; morphometry; primary cell culture; retinal pigment epithelium; serum content; coating

Academic Editor: Wolfgang Graier

Received: 5 November 2024
Revised: 28 January 2025
Accepted: 5 February 2025
Published: 10 February 2025

Citation: Dörschmann, P.; Wilke, J.; Tietze, N.; Roider, J.; Klettner, A. Single-Eye Porcine Retinal Pigment Epithelium Cell Cultures—A Validated and Reproducible Protocol. *BioMed* **2025**, *5*, 7. https://doi.org/10.3390/biomed5010007

1. Introduction

Reliable ocular cell models for the research of ophthalmologic diseases are highly warranted. One of these diseases is age-related macular degeneration (AMD), the main cause of severe central vision loss in the elderly and Western nations, with increasing patient numbers expected to go up to 288 million by 2040 [1]. Early forms of AMD are without symptoms, whereas the two late forms lead to severe vision disturbance. In the late dry form, atrophy develops in the retinal pigment epithelium (RPE) and photoreceptors, while in the exudative (wet) form of late AMD, VEGF is oversecreted and blood vessels grow from the choroid under and into the retina [2]. Molecular pathomechanisms in the

development of AMD are oxidative stress, inflammation, lipid dysregulation, and proangiogenic factors [3]. These are primarily targeting RPE within the photoreceptor/RPE/Bruch's membrane/choriocapillaris complex [4]. The RPE maintains visual functions by supplying nutrients, taking up waste, forming the outer blood–retinal barrier, contributing to the immune privilege, phagocyting shed photoreceptor outer segments, releasing protective chemokines, and protecting against light and oxidative stress [5]. The RPE is supported by an extracellular structure known as Bruch's membrane, which consists of collagen Type IV, fibronectin, and laminin [6]. These substances are also used for the coating of cell culture plates.

For a better understanding of all underlying physiological cell functions and pathways involved in the development of ocular diseases, or to develop new therapeutics, optimized and conclusive cellular model systems are highly desired. For an overview, the reader is referred to current comprehensive reviews [7,8]. Cell lines, like the human RPE cell line ARPE-19, are frequently used but differ considerably from a differentiated RPE cell in terms of morphology, barrier function, or gene expression [7,9–11]. There are published protocols that can induce a more RPE-like differentiation of ARPE-19 cells (e.g., [12] or [13]), but mostly, ARPE-19 cell culture protocols are implemented for fast results. Furthermore, these transformed, immortal cells have been passaged for years and have changed their characteristics [14,15]. Many researchers now rely on induced pluripotent stem cell (iPSC)-derived RPE cells from human donors. While these have the great advantage of being human, an iPSC-derived RPE cell also has its difficulties. Cultures of RPE derived from iPSC show subpopulations with different levels of maturity and gene expression with high variability, even within a single culture, including the population of stem cell-like progenitors and cells specialized for different RPE functions in the same culture or cultures from the same donor displaying either fetal or adult characteristics [16–19]. In addition, iPSC-derived cells may contain epigenetic modifications that are not found in natural RPE cells [20]. However, in spite of these challenges, iPSC-derived stem cells also have advantages compared to porcine cell models (see below), not only because of their human origin but also because of the possibility to use harvested patient material, giving the opportunity to directly investigate the impact of, e.g., genetic variants of patients on cell behavior and pathology development [21,22]. Furthermore, they can be developed for RPE transplantation [17,23]. Both are features that cannot be modeled by porcine cells. Mice are also widely used in retinal research. However, the use of mice to study diseases like AMD has severe disadvantages. Mice are nocturnal animals with very small eyes. Mice have very low visual acuity with no area of high(er) acuity vision, rely mainly on rods, express cones not found in humans (ultraviolet and double cones), and show features, such as an inverted rod chromatin structure, that are not found in humans [7]. Furthermore, their RPE is rather different from the human situation, with a high percentage of multi-nucleated RPE cells and different claudins used in their tight junctions [24,25]. In contrast, pigs are diurnal animals with eyes of similar size and anatomic features resembling the human eye; their eyes rely highly on cone vision with an area of higher visual acuity found in the retina (area centralis). Their cones resemble human blue and red/green cones (the division between red and green has only happened in primates), and they show the same degree of multi-nucleus characteristics and the same claudins in tight junctions as humans [7,24–27]. Despite the relevance of the porcine RPE as a model for human diseases, there are limitations to the use of this model. While the pig resembles the human situation much more closely than the mouse, it is still not identical to the human situation [7,27]. As pointed out above, porcine material cannot be used for transplantation. Furthermore, pigs, like all non-primate mammals, do not contain a macula, and SNPs related to AMD development are not described in the pig. Another limitation of using the pig as a model

is the limited availability of analytics, such as primers or antibodies, which are readily available for mice and humans. Furthermore, creating transgenic animals, while possible in the pig [28,29], is cheaper and more easily performed in the mouse. Finally, housing conditions are much more expensive for pigs compared to mice.

However, the availability of porcine eyes as waste products makes them easily available without the need to house, breed, and kill animals purely for scientific purposes. Their use is, therefore, an active contribution to the 3R principle. Indeed, porcine cells are frequently used, and several protocols are available. In all published protocols, however, RPE cells of different eyes are usually mixed (e.g., [30–34]), so that cultures contain cells of different genetic origins, which implies different responses in one cell culture.

This study aims to generate a standardized and optimized operation protocol for the preparation of porcine RPE single-eye cultures. Here, the RPE cells from one pig eye are seeded into one well of a twelve-well polystyrene plate. This is in contrast to the usual protocols in which RPE cells from several eyes are mixed before seeding. The conventional protocols create genetically heterogeneous cultures where certain effects may be confounded by the heterogeneity of the cells. With single-eye cultures, each culture (or well of a plate) is genetically homogeneous, resembling an individual. At the same time, the cultures are genetically heterogeneous between the separate cultures (or wells). This setting will potentially generate scientific data more relevant to the real-life situation, as it resembles the human situation much closer. Also, with the use of porcine eyes from waste material in the food industry, animal experiments can be avoided, contributing to the 3R principle [30]. Furthermore, porcine material is far closer to the human eyes compared to the widely used mouse eye models, as described above. In addition, porcine RPE can be prepared after short post-mortem times (PMT), does not need characterization, and is extremely economical compared to human or stem-cell-derived RPE [31].

A new single-eye porcine RPE cell model with potentially higher biological relevance would, therefore, be a cost-effective and reproducible model that could be globally applied in research targeting RPE-based diseases, such as AMD. This model can be used to address specific classical pathology-related aspects, such as oxidative stress, inflammation, or proangiogenic signaling [3,8], but also lesser investigated pathways, such as RPE epithelial–mesenchymal transformation in subretinal fibrosis [32] or autophagy [33]. In addition, the homogenous genetic background of the RPE cell culture renders these cells highly suitable for proteomic or gene expression studies in pathogenic AMD pathways [34]. In addition, the data we present can be used as a basis for establishing quality control in porcine cell culture, especially considering cell morphology and morphometry.

Parameters that are important for the efficiency, differentiation, and expression of the RPE are PMT, plate coating substances, and the serum level of the medium. The outcome parameters of this study are cell number, confluency, morphology, differentiation, protein, and gene expression, as well as VEGF secretion. In addition, basic morphometric data were established for porcine RPE cells. For these parameters, a standard basic protocol for optimized preparation and cultivation was generated and is provided in this study. The overall experimental set up is depicted in Figure 1.

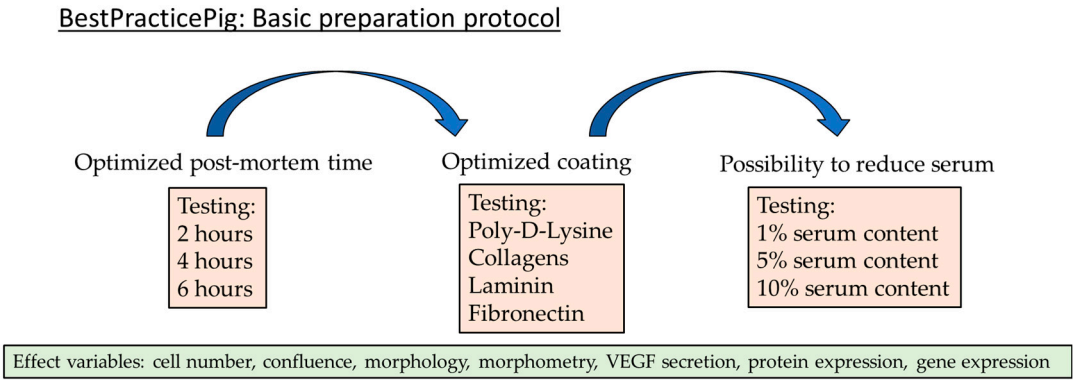

Figure 1. Flowchart of the experimental set up. The aim of this study is to establish a basic protocol for the preparation of porcine retinal pigment epithelial cells (RPE) as a single-eye culture model. The RPE cells of one eye are seeded into one well of a twelve-well plate. The preparation parameters post-mortem time, coating of the well plates, and serum content are tested and optimized. The results are analyzed with regard to cell numbers, confluence, morphology/morphometry, and the secretion and expression of various RPE markers.

2. Materials and Methods

2.1. Cell Culture

All RPE cultures were prepared from freshly slaughtered pigs' eyes at 2 to 6 h PMT. All pigs were examined by veterinarians and were used for food production; therefore, they can be considered disease free. Pigs from Deutsche Landrasse race, mixed sex, and ages of 5 to 6 months were used.

The use of these eyes for experimental purposes was conducted in agreement with the animal welfare officer of the University of Kiel. According to the German Animal Welfare Act (TierSchG, https://www.gesetze-im-internet.de/tierschg (accessed on 8 February 2025). This is not considered to be animal research, but an alternative to the use of animals in research. The overall method is based on the preparation of RPE from mixed cultures [35] and was adapted to seed RPE cells from one eye into one well of a twelve-well polystyrene plate for adherent cells (Sarstedt, Nümbrecht, Germany; #83.3921) with a growth area of 3.65 cm^2 and a culture medium volume of 1 mL. A detailed protocol can be found in the Appendix B. All RPE cells harvested from one pig eye were seeded into one well of one twelve-well plate. The time difference between the first and the last eye of the 12-eye batch was ten minutes.

In brief, adjacent tissue was removed and the eyes were disinfected with betaisodona (Mundipharma, Germany; Frankfurt am Main, Germany; #04923204) and washed with 0.9% NaCl (Fresenius Kabi, Bad Homburg, Germany; #04801702), both on ice. The cornea, iris, ciliary body, and vitreous body were removed under aseptic conditions. The retina was detached in sterile Dulbecco's phosphate-buffered saline without Ca^{2+} and Mg^{2+} (DPBS, Pan-Biotech, Aidenbach, Germany; #P04-53500) plus 1% penicillin/streptomycin (Pe/St, Sigma-Aldrich, St. Louis, MO, USA; #P0781). RPE cells were incubated for 10 min with 0.25% trypsin (Pan-Biotech; #P10-021100), followed by a 35 min incubation in 0.25% trypsin/0.02% ethylenediaminetetraacetic acid (EDTA, Pan-Biotech; #P10-020100). Cells from one eye were collected in a 15 mL tube (Sarstedt; #62.554.502), filled with 5 mL standard RPE media. Standard RPE media consists of Dulbecco's Modified Eagle Medium with high glucose, L-glutamine, and phenol red (DMEM, Gibco™, Thermo Fisher Scientific, Waltham, MA, USA; #41965062), supplemented with 1% non-essential amino acids (Pan-Biotech; #P08-32100), 11 mM sodium pyruvate (Pan-Biotech; #P04-43100), 1% Pe/St, and 10% fetal bovine serum (FBS Mexican origin, Gibco™, Thermo Fisher Scientific; #10437028, Lot: 2405703RP). For serum testing assays, three days after preparation, the concentration

of serum was changed from 10% to 5% or 1%, respectively. Cells were washed twice in 5 mL media (centrifugation), and the pellet was suspended in 1 mL media and seeded into one well of a twelve-well plate. The cells were incubated at 37 °C and 5% CO_2 in a humidified incubator. The protocol for the preparation process is provided (Appendix B).

To assess barrier function, single-eye RPE were seeded on twelve-well plates with uncoated transwell inserts (Sarstedt; #83.3931.041) and cultured for 28 days in media containing 10% FBS. Transepithelial electrical resistance (TEER) was measured with an EVOM3 Epithelial Volt/Ohm (TEER) Meter (World Precision Instruments Germany GmbH, Friedberg, Germany) after 7, 14, and 28 days.

As season may influence the quality of the eyes, we present the months in which the specific experiments were conducted. Tests regarding the qualities of the eyes and post-mortem times were conducted from May to November 2022, whereas actin evaluation samples were prepared from July to October. Coating tests with collagens were conducted from November to December 2022. Other coatings were tested from January to June 2023, whereas samples for tight junction assessment were prepared from March to September 2023. Serum content tests were conducted from May to September 2023, whereas samples for tight junction staining were prepared from August to September 2023.

2.2. Coating

Different coatings were applied on individual wells of twelve-well plates. Collagen Type I in monomeric (CIm) or fibrillar (CIf) form (Collagen A, 1 mg/mL, Pan Biotech, Aidenbach, Germany; #P06-20030), collagen Type IV (CIV, Advanced Biomatrix, Inc., Carlsbad, CA, USA; #5022), laminin (La, Sigma-Aldrich; #11243217001), fibronectin (Fn, Advanced Biomatrix; #5080), or Poly-D-Lysine (PDL, Sigma-Aldrich; #P7886) were used. All substances were applied as described in the manufacturers' instructions with recommended concentrations (CIm/CIf—1 mg/mL or 100 µg/cm^2, CIV—100 µg/mL or 10 µg/cm^2, La—20 µg/mL or 2 µg/cm^2, Fn—50 µg/mL or 5 µg/cm^2, PDL—100 µg/mL or 10 µg/cm^2) and a well volume of 365 µL (100 µL/cm^2 well).

2.3. Trypan Blue Exclusion Assay and Light Microscopy

Cells from one eye or one well, respectively, were counted before seeding (one eye) and after specific culture times (one well). For this, adherent cells were detached with trypsin/EDTA incubation; a 20 µL cell suspension was collected, mixed with 20 µL 0.4% trypan blue solution (Sigma-Aldrich; #T8154), and incubated for 3 min. The mixture was applied to a Neubauer counting chamber (Carl Roth GmbH + Co. KG, Karlsruhe, Germany; #T729.1). Cells were counted in a bright field using an Axiovert 160 (Carl Zeiss AG, Oberkochen, Germany) microscope with a 10× objective. The same microscope was used to take pictures of the cells to assess the morphology after 7, 14, and 28 days of cultivation. The photos were taken at distinct coordinates at the center, the middle ring, and the outer border of the wells using Axiovision Release 4.8.0.0 (Carl Zeiss AG). The percentage of epithelial, mesenchymal, and undivided cells, as well as gaps, were determined by a researcher. Also, confluence in percent 7 days after seeding as well as the day of 95–100% confluence was determined.

2.4. Enzyme-Linked Immunosorbent Assay

Secreted VEGF-A was determined with ELISA. For this, supernatants of single-eye culture RPE were collected for 4 h, centrifuged, and stored at −20 °C. These samples were assessed in Human VEGF DuoSet ELISA (R&D systems, Minneapolis, MN, USA; #DY293B) as described by the manufacturer.

2.5. Fluorescence Imaging—Tight Junctions and Cell Parameters

The labeling of actin filaments, cell nuclei, and tight junctions (zonula occludens 1, ZO-1) was performed on cells seeded on coverslips (Th. Geyer GmbH & Co. KG, Renningen, Germany; #CB00180RA1). Cells were fixated in 3% para-formaldehyde (Carl Roth GmbH + Co. KG; #0335.1) and permeabilized with 0.1% Triton-X (Carl Roth GmbH + Co. KG; #3051.2). Cells were blocked with 3% BSA diluted in PBS for one hour (Thermo Fisher Scientific; #37525). After blocking, cells were incubated for one hour with rabbit ZO-1 polyclonal antibody (Thermo Fisher Scientific; #61-7300, diluted 1:50), followed by a one-hour incubation with a secondary antibody mixture containing Hoechst (Sigma-Aldrich; #14533, diluted 1:500), Phalloidin-Atto488 (Sigma-Aldrich; #49409, diluted 1:50), and Alexa Fluor 555 goat anti-rabbit (Thermo Fisher Scientific; #A32732, diluted 1:1000). Coverslips were mounted with Fluoromount-G (Thermo Fisher Scientific; #00-4958-02) on microscope slides (Th. Geyer GmbH & Co. KG; #42406010). Fluorescence images were taken with a fluorescence microscope Imager.M2 (Carl Zeiss AG) with a 20× objective. At least three pictures from different positions were taken per coverslip. The quality of the actin filaments and tight junctions for each set of experiments were assessed by a single researcher, blinded to the conditions. For actin experiments, cell nuclei were evaluated using Fiji (Image J2). The ZO-1 signal as well as cell nuclei were evaluated with CellProfiler Software, version 4.2.8. (Broad Institute of MIT and Harvard). These data were used to determine cell parameters (cell and nuclei number, cell area, cell perimeter, eccentricity, form factor, and cell radius).

2.6. Quantitative Polymerase Chain Reaction

RNA was isolated after 28 days of cultivation in different conditions (PDL or no coating, respectively, combined with 10% or 5% serum, respectively) with a NucleoSpin RNA Mini Kit and digested with DNase (Macherey-Nagel, Düren, Germany; #740955), according to manufacturer's instructions. RNA quality and concentration were determined with NanoDrop™ One (Thermo Fisher Scientific; #ND-ONE-W). cDNA was generated with the High-Capacity cDNA Reverse Transcription Kit (Thermo Fisher Scientific; #4368814) as described in the manual. Real-time qPCR was performed with TaqMan™ gene expression assays (Thermo Fisher Scientific; #4351372) and TaqMan™ Fast Advanced Master Mix (Thermo Fisher Scientific; #4444557) as described in the manual for the master mix. Also, self-designed gene arrays for RPE-relevant porcine genes were applied containing 96 different gene targets with dye label 5(6)-carboxyfluorescein-minor groove binder (FAM-MGB) [36]. Endogenous controls *ACTG*, *GAPDH*, and *GUSB* were used for normalization. 18s rRNA was used as manufacturing control by Thermo Fisher Scientific. The design of the gene array is depicted in Table 1. For the calculation of relative gene expression, the ΔΔCT method was used [37]. ΔCT [=CT (gene of interest) − CT (housekeeping gene)], ΔΔCT [=ΔCT (treated sample) − ΔCT (untreated sample)] and the relative fold gene expression level RQ (=2 ΔΔCT) were assessed with Thermo Fisher Connect (RQ module, relative quantification).

Table 1. Gene array design. Gene targets with well position and gene expression ID are shown, including the name of the encoded gene product. Underlined targets were used as endogenous controls.

Well	Target	Product	Assay ID
A1	18s rRNA	18s rRNA (Human)	Hs_99999901_s1
A2	*ABCA4*	ATP-Binding Cassette Subfamily A Member 4	Ss06884373_m1
A3	*ACTG*	Actin, Cytoplasmic 2	Ss03376081_u1
A4	*ADRB2*	Adrenoceptor Beta 2	Ss03818941_s1
A5	*ANGPT2*	Angiopoietin 2	Ss03392362_m1

Table 1. *Cont.*

Well	Target	Product	Assay ID
A6	*ANGPTL2*	Angiopoietin-Like 2	Ss03389615_m1
A7	*ANXA5*	Annexin A5	Ss06880508_m1
A8	*APOE*	Apolipoprotein E	Ss03394681_m1
A9	*BDNF*	Brain-Derived Neurotrophic Factor	Ss03822335_s1
A10	*BEST1*	Bestrophin 1	Ss03376235_u1
A11	*C2*	Complement C2	Ss03389255_m1
A12	*C3*	Complement C3	Ss03391255_m1
B1	*C5*	Complement C5	Ss03391586_m1
B2	*C9*	Complement C9	Ss03388866_m1
B3	*CASP1*	Caspase 1	Ss03394224_m1
B4	*CAT*	Catalase	Ss04323025_m1
B5	*CCL2*	C-C Motif Chemokine Ligand 2	Ss03394377_m1
B6	*CCL5*	C-C Motif Chemokine Ligand 5	Ss03648939_m1
B7	*CD46*	CD46 Molecule	Ss03392461_u1
B8	*CD55*	CD55 Molecule (Cromer Blood Group)	Ss03392383_m1
B9	*CD59*	CD59 Glycoprotein (Protectin)	Ss03394252_m1
B10	*CFB*	Complement Factor B	Ss03389385_g1
B11	*CFH*	Complement Factor H	Ss03391439_m1
B12	*CFI*	Complement Factor I	Ss06935384_m1
C1	*COL14A1*	Collagen Type XIV Alpha 1 Chain	Ss06865093_m1
C2	*CRP*	C-Reactive Protein	Ss03390889_m1
C3	*CRYAA (CRYA1)*	Crystallin Alpha A	Ss06837084_m1
C4	*CRYAB*	Alpha-Crystallin B Chain	Ss06921086_m1
C5	*CSF2*	Colony-Stimulating Factor 2	Ss03394096_m1
C6	*CST3*	Cystatin C	Ss03388477_m1
C7	*CTSD*	Cathepsin D	Ss03379762_u1
C8	*CX3CR1*	CX3C Chemokine Receptor 1	Ss06883230_m1
C9	*CXCL10*	C-X-C Motif Chemokine Ligand 10	Ss03391846_m1
C10	*CXCL12*	C-X-C Motif Chemokine Ligand 12	Ss03391855_m1
C11	*DICER1*	Dicer 1, Ribonuclease III	Ss04248150_m1
C12	*ELN*	Elastin	Ss04955056_m1
D1	*FASLG*	Fas Ligand	Ss03381579_u1
D2	*FLT1*	Fms-Related Tyrosine Kinase 1 (VEGF-R1)	Ss03375679_u1
D3	*FMO1*	Flavin-Containing Dimethylaniline Monoxygenase 1	Ss03393883_u1
D4	*FN1*	Fibronectin 1	Ss03373673_m1
D5	*FST*	Follistatin	Ss03378467_u1
D6	*GAPDH*	Glyceraldehyde-3-Phosphate Dehydrogenase	Ss03375629_u1
D7	*GFAP*	Glial Fibrillary Acidic Protein	Ss03373547_m1
D8	*GPX4*	Glutathion Peroxidase 4	Ss03384646_u1
D9	*GSS*	Glutathione Synthetase	Ss04328106_m1
D10	*GUSB*	Glucuronidase Beta	Ss03387751_u1
D11	*HIF1A*	Hypoxia-Inducible Factor 1 Subunit Alpha	Ss03390447_m1
D12	*HMOX1*	Heme Oxygenase 1	Ss03378516_u1
E1	*HTRA1*	HtrA Serine Peptidase 1	Ss06876775_m1
E2	*ICAM-1*	Intercellular Adhesion Molecule 1	Ss03392385_m1
E3	*IGF1*	Insulin-Like Growth Factor 1	Ss03394499_m1
E4	*IL1B*	Interleukin 1 Beta	Ss03393804_m1
E5	*IL1R2*	Interleukin 1 Receptor Type 2	Ss04324011_m1
E6	*IL6*	Interleukin 6	Ss07308316_g1
E7	*Il6R*	Interleukin 6 Receptor	Ss03394904_g1
E8	*IL8 (=CXCL8)*	Interleukin-8 (CXCL-8)	Ss03392437_m1
E9	*KDR*	Kinase Insert Domain Receptor (VEGF-R2)	Ss03375683_u1
E10	*KIT*	KIT Proto-Oncogene, Receptor Tyrosine Kinase	Ss03380145_u1
E11	*LEP*	Leptin	Ss03392404_m1
E12	*LIPC*	Lipase C	Ss03820991_s1
F1	*LPL*	Lipoprotein Lipase	Ss03394608_m1
F2	*MAPK1*	Mitogen-Activated Protein Kinase 1 (ERK2)	Ss04248225_m1
F3	*MAPK14*	Mitogen-Activated Protein Kinase 14 (p38)	Ss06880885_m1
F4	*MMP2*	Matrix Metallopeptidase 2	Ss03394318_m1
F5	*MMP9*	Matrix Metallopeptidase 9	Ss03392100_m1

Table 1. *Cont.*

Well	Target	Product	Assay ID
F6	*MTOR*	Mechanistic Target Of Rapamycin Kinase	Ss03377427_u1
F7	*NFE2L2*	Nuclear Factor, Erythroid 2 Like 2 (NRF2)	Ss06886076_m1
F8	*NKAP*	NFKB-Activating Protein	Ss04322419_m1
F9	*NOS1*	Nitric Oxide Synthase 1	Ss06838170_m1
F10	*NOS2*	Nitric Oxide Synthase 2 (iNOS)	Ss03374608_u1
F11	*PLA2G2D*	Phospholipase A2 Group IID	Ss04953157_m1
F12	*PTGS1*	Prostaglandin–Endoperoxide Synthase 1	Ss03373347_m1
G1	*PTGS2*	Prostaglandin–Endoperoxide Synthase 2 (COX2)	Ss03394694_m1
G2	*RDH11*	Retinol Dehydrogenase 11	Ss06878003_m1
G3	*RLBP1*	Retinaldehyde-binding protein 1	Ss06905574_m1
G4	*RPE65*	Retinoid Isomerohydrolase RPE65	Ss06891920_m1
G5	*SCARB1*	Scavenger Receptor Class B Member 1	Ss03391104_m1
G6	*SERPINF1*	Serpin Family F Member 1	Ss03385090_u1
G7	*SERPING1*	Serpin Family G Member 1	Ss03387977_u1
G8	*SOD1*	Superoxide Dismutase 1	Ss03375614_u1
G9	*SOD2*	Superoxide Dismutase 2	Ss03374828_m1
G10	*SPARC*	Secreted Protein Acidic And Cysteine Rich	Ss03392006_m1
G11	*TF*	Transferrin	Ss03374732_m1
G12	*TGFB1*	Transforming Growth Factor Beta 1	Ss04955543_m1
H1	*TIMP1*	TIMP Metallopeptidase Inhibitor 1	Ss03381944_u1
H2	*TIMP-3*	TIMP Metallopeptidase Inhibitor 3	Ss03375447_u1
H3	*TLR2*	Toll-Like Receptor 2	Ss03381278_u1
H4	*TLR3*	Toll-Like Receptor 3	Ss03388862_m1
H5	*TLR4*	Toll-Like Receptor 4	Ss04956023_s1
H6	*TNF*	Tumor Necrosis Factor	Ss03391318_g1
H7	*TYR*	Tyrosinase	Ss03379283_u1
H8	*VCAM1*	Vascular Cell Adhesion Molecule 1	Ss03390912_m1
H9	*VEGFA*	Vascular Endothelial Growth Factor A	Ss03393990_m1
H10	*VIM*	Vimentin	Ss04330801_gH
H11	*VLDLR*	Very Low-Density Lipoprotein Receptor	Ss03374049_m1
H12	*VWF*	Von Willebrand Factor	Ss04322692_m1

2.7. Protein Expression

Western blotting was performed to assess claudin-19 (CLDN19) and retinal pigment epithelium-specific 65 kDa protein (RPE65) expression. After 2 or 4 weeks of cultivation, cells were washed with PBS and lysed with Nonidet P40 solution (NP40) containing 1% Nonidet P40 Substitute (Sigma-Aldrich; #11332473001), 150 mM NaCl (Carl Roth GmbH + Co. KG; #3957.1), and 50 mM Tris (Sigma-Aldrich; #T1503, pH8) and supplemented with phosphatase inhibitor cocktail 1 and 2 (Sigma-Aldrich; #P2850, #P5726) as well as protease inhibitor cocktail (Sigma-Aldrich; #P8340) for 45 min. Protein content was assessed with DC Protein Assay (Bio-Rad Laboratories, Munich, Germany; #5000111), according to the manufacturer's instructions. SDS-PAGE and Western blotting were conducted as previously described, with modifications [38]. A 12% acrylamide gel was used. PageRuler™ Plus Prestained Protein Ladder (Thermo Fisher Scientific; #26620), with a range of 10 to 250 kDa, was applied. Membranes were blocked with 4% skimmed milk (Carl Roth GmbH + Co. KG; #T145.2) in Tris-buffered saline with 0.05% Tween (TBST, Merck KGaA, Darmstadt, Germany; #8221840) for one hour. Membranes were incubated with primary antibodies overnight, rocking at 4 °C (mouse anti-RPE65, 65 kDa, 1:2000 in 2% skimmed milk, Novus Biologicals, Minneapolis, MN, USA; #NB100-355; rabbit anti-CLDN19, 23 kDa, 1:1000 2% skimmed milk, Absource Diagnostics GmbH, München, Germany; #00219; rabbit anti-β-actin, 37 kDa, 1:1000 in 2% skimmed milk, Cell Signaling Technologies, Denver, CO, USA, #4967). After several washing steps with TBST, secondary antibody conjugates were applied for one hour (horseradish peroxidase-conjugates, HRP, anti-mouse-HRP (Cell Signaling Technologies; #7076), anti-rabbit-HRP (Cell Signaling Technologies; #7074),

both 1:1000 in 2% skimmed milk). For the chemiluminescence signal, Clarity Western ECL Substrate (Bio-Rad Laboratories; #170-5061) was applied for 5 min. The signal was detected with a ChemiDoc MP Imaging System (Bio-Rad Laboratories). Band volumes were normalized with β-actin expression and evaluated with Image Lab 6.1.0 build 7 software (Bio-Rad Laboratories).

2.8. Statistical Analysis

All experiments were independently conducted at least three times. Data management, diagrams, and calculations were carried out using Microsoft Excel (Excel 2010, Microsoft, Redmond, WA, USA). qPCR data were evaluated with the cloud software Thermo Fisher Connect. Statistical analysis was performed with GraphPad Prism 9 (GraphPad Software, Inc., San Diego, CA, USA, 2021) and Thermo Fisher Connect for the PCR data. Parametric distribution was assessed with the Shapiro–Wilk test. The significance of parametric data was determined with ANOVA (analysis of variance) and Student's *t*-test; the significance of non-parametric data was determined with the Kruskal–Wallis and Mann–Whitney tests. The error bars of the column charts show the standard deviation. The bars of the box plots range from lowest (minimum) to highest values (maximum). For transparency regarding the range of data, an overview of parametric data with the mean, standard deviation, minimum, and maximum is listed in Table A3 (Appendix A). Also, individual data points of parametric data are shown. PCR data were evaluated with Student's *t*-test calculated with Thermo Fisher Connect. Data were considered significant with p-values < 0.05. The number of experiments n represents the number of individual eyes used for the experiments.

3. Results

3.1. Quality of the Eyes and Post-Mortem Time

3.1.1. Qualities of the Eyes

In order to assess the barrier function of single-eye cultures, RPE cells were seeded on 12-transwell plates, and TEER was measured after 7, 14, and 28 days of cultivation (Figure 2). All cells were seeded on uncoated wells and fed with media containing 10% serum. Cells reached a TEER of 228 ± 110 Ω*cm^2, 315 ± 116 Ω*cm^2, and 497 ± 315 Ω*cm^2 after 7, 14, and 28 days, respectively. These high TEER values confirm that the single-eye cultures form a strong barrier. Further assays of this study were conducted with twelve-well plates without transwell inserts.

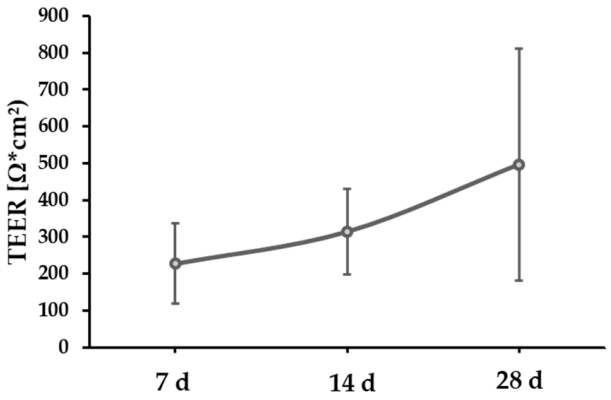

Figure 2. Barrier measurement of porcine retinal pigment epithelium single-eye cultures. Single-eye porcine cultures were seeded on 12-transwell plates and cultured for 28 days. Transepithelial electrical resistance (TEER) in Ω*cm^2 was measured after 7, 14, and 28 days. n = 24.

Freshly slaughtered pigs' eyes can be of different qualities when they reach the laboratory. Their cornea and lens can be bleared or clear, depending on the time the pigs

were scalded before the eyes were removed, which may denature the proteins of the cornea and the lens as seen in bleared eyes. Data for testing post-mortem times (PMTs) were collected and summarized for all PMTs (2, 4, and 6 h) and evaluated concerning bleared and clear eyes (Figures 3 and 4). Eyes with light-reflecting effects or a blue iris were not used for preparation as they contained fewer (pigmented) RPE cells. Data were evaluated for cell number after 7, 14, and 28 days (Figure 3A), number of days to reach 95–100% confluency (Figure 3B), confluency in % on day 7 of cultivation (Figure 3C), and success rates for survival and confluence (Figure 3D). Clear eyes reached a cell number of 7.91 ± 3.18 cells × 10^5/mL, 8.37 ± 3.83 cells × 10^5/mL, and 8.70 ± 3.78 cells × 10^5/mL after 7, 14, and 28 days, respectively. Bleared eyes reached a cell number of 7.96 ± 3.33 cells × 10^5/mL, 8.58 ± 3.83 cells × 10^5/mL, and 9.54 ± 3.02 cells × 10^5/mL after 7, 14, and 28 days, respectively. The day of confluence for clear eyes was day 8.00 ± 3.00, and for bleared eyes, it was day 10.00 ± 3.00. Confluence on day 7 was 95.00% ± 40.00% for clear eyes and 82.50% ± 50.00% for bleared eyes. Clear eyes showed a death rate of 25.26% and a confluence rate of 60.00%, and bleared eyes showed a death rate of 24.11% and a confluence rate of 56.74%. Overall, no significant differences were found, but the values concerning confluency were better with clear eyes.

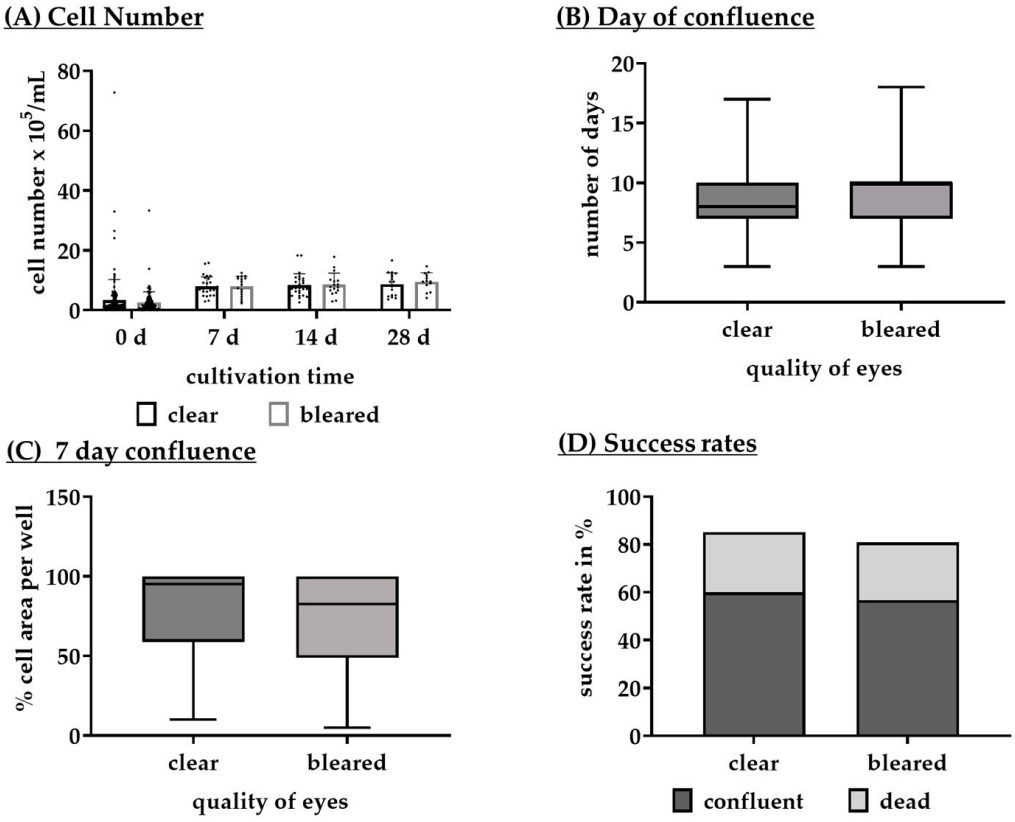

Figure 3. Influence of the qualities of porcine eyes on different parameters. Data to test post-mortem times were collected and evaluated regarding the quality of the porcine eyes divided into clear and bleared eyes. They were evaluated for cell number ((**A**), *n* = 13–165), day when they reach 95–100% confluence ((**B**), *n* = 81–113), confluence in % on day 7 ((**C**), *n* = 94–126) of cultivation, and rates for dead and confluence cultures ((**D**), *n* = 34–190). Data for (**A**) were parametric; mean and standard deviation are depicted. Significances were calculated between each group with analysis of variance (ANOVA) and Student's *t*-test. Data for (**B**,**C**) was not parametric; median and interquartile ranges are depicted. Significances were calculated between each group with the Kruskal–Wallis test and Mann–Whitney tests. No significant differences were found. Data for (**D**) are descriptively shown as stacked bars with a percentage ratio. d = days.

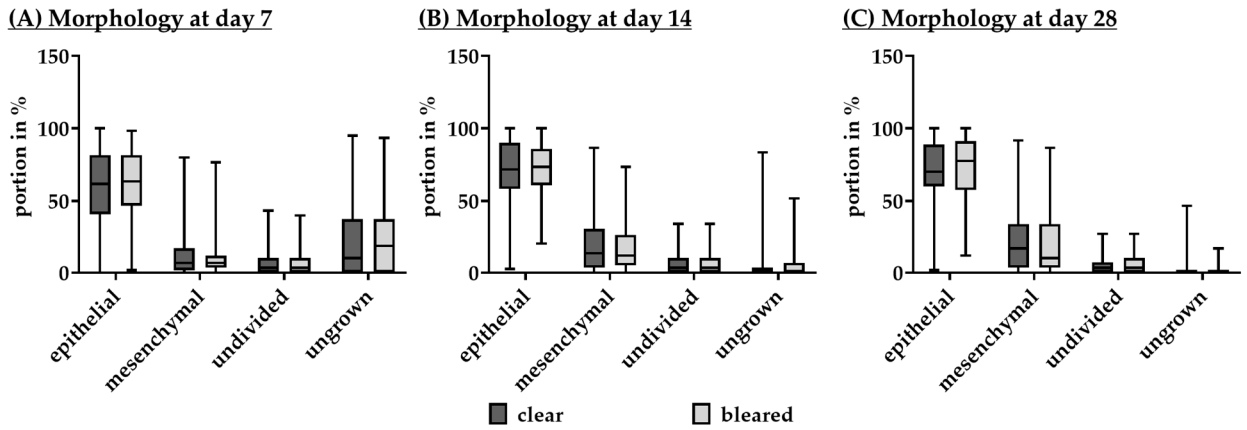

Figure 4. Influence of the qualities of porcine eyes on different culture parameters. Single-eye retinal pigment epithelium cells were seeded for seven ((**A**), n = 126–129), 14 ((**B**), n = 94–95), and 28 days ((**C**), n = 50–53). A portion of epithelial, mesenchymal, undivided cells, and ungrown areas of clear or cleared eyes was determined with light microscopy after incubation. Data were not parametric; median and interquartile ranges are depicted. Significances were calculated between each group with the Kruskal–Wallis test and the Mann–Whitney test. No significances were detected.

Also, cell morphology was determined after 7 (Figure 4A), 14 (Figure 4B), and 28 days (Figure 4C) of cultivation. Light microscopy images of different areas of the well were visually analyzed for the proportion of epithelial, mesenchymal, and undivided cells, as well as ungrown areas, all as % portions of 100% well area. Data were again very similar between qualities (please refer to Table A1 in Appendix A). Regarding the entire data set, the % of undivided cells between day 7, day 14, and day 28 remained the same at 3.33% at all time points. Ungrown areas were filled up over time, decreasing from 12.50% to 0.00%. These areas were filled up both with mesenchymal cells (from 6.67% to 11.67% and 13.33%, respectively) and epithelial cells (from 63.33% to 72.50% and 73.33%, respectively).

All data were very similar and showed no significant or relevant differences. For the following assays, it was assumed that these qualities (clear, bleared) would not confound the results.

3.1.2. Post-Mortem Time

Single-eye RPE cells were prepared after a PMT of 2, 4, and 6 h and cultivated for 7, 14, and 28 days. Cell number after respective cultivation time (Figure 5A), the number of days until reaching 95–100% confluence (Figure 5B), confluence area on day 7 of cultivation (Figure 5C), and overall survival and confluence success rates were determined (Figure 5D).

Regarding cell numbers, data for all PMT were summarized and descriptively evaluated concerning seeding cell number and success of the culture (Table 2). A living and successful culture was defined as containing cells that were quantifiable in a trypan blue exclusion assay (showing a living cell number of at least 0.05×10^5 cells/mL) over the course of 28 days of cultivation. Overall, the mean and median cell seeding numbers between successful (living) and unsuccessful (dead) cultures were not relevantly different. However, a seeding cell number of at least 1×10^5 cells/mL increased the success rate, as in dead cultures, cell number was more often below 1×10^5 cells/mL than in succeeding cultures (61.70% compared to 28.39% for living cultures).

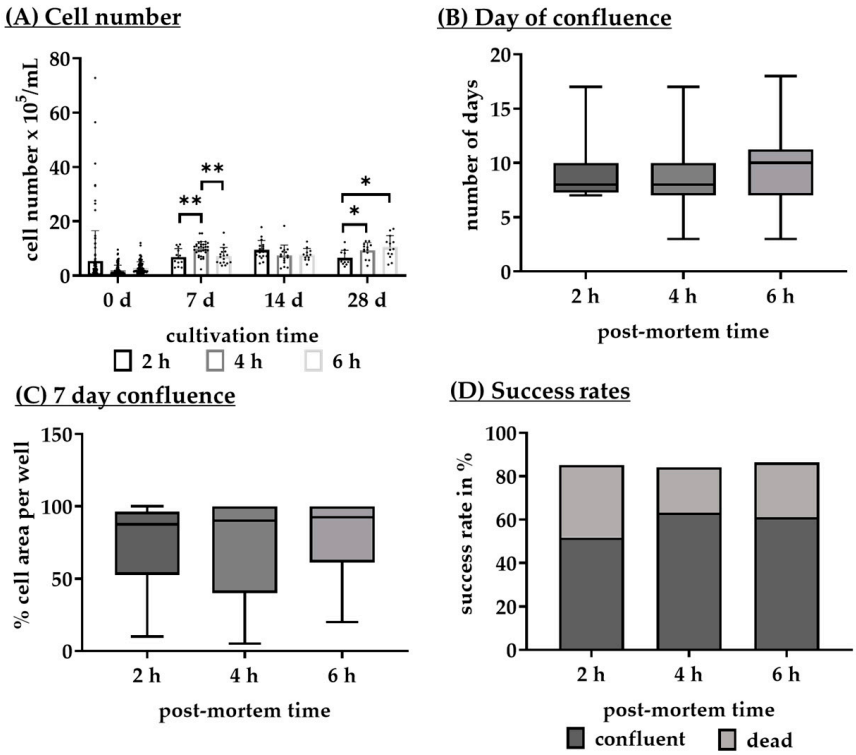

Figure 5. Influence of post-mortem time on different culture parameters. Single-eye retinal pigment epithelium cells were prepared after 2, 4, and 6 h post-mortem time and seeded for 7, 14, and 28 days. After different cultivation times, cells were counted ((**A**), n = 11–112), the number of days until reaching 95–100% confluence was determined ((**B**), n = 56–91), a confluence area on day 7 of cultivation was estimated ((**C**), n = 66–94), and the overall survival and confluence success rates were determined ((**D**), n = 108–143). Data for (**A**) were parametric; mean and standard deviation are depicted. Significances were calculated between each group with analysis of variance (ANOVA) and Student's t-test. Data for (**B**,**C**) were not parametric; median and interquartile ranges are depicted. Significances were calculated between each group with the Kruskal–Wallis test and Mann–Whitney tests. Data for (**D**) are descriptively shown as stacked bars with a percentage ratio. * $p < 0.05$, ** $p < 0.01$, h = hours, d = days.

Table 2. Descriptive analyses of summarized cell seeding number data. Numbers are depicted as $\times 10^5$ cells/mL. Min = minimum; Max = maximum.

	Total	Living	Dead
Mean	3.55	3.80	2.28
Deviation	7.16	6.91	8.25
Median	1.65	2.00	0.75
Range	72.80	71.75	56.45
Min	0.00	0.05	0.00
Max	72.80	72.80	56.45
Count total (n)	283.00	236.00	47.00
% <1.00	33.92%	28.39%	61.70%
% >1.00	66.08%	71.61%	38.30%

Concerning the influence of PMT, seeding cell number after 2 h PMT showed high variation. After 7 days of cultivation, 4 h PMT showed the highest cell number (mean: 9.85 ± 2.69 cells × 10^5/mL), which was significantly higher than 2 h PMT (mean: 6.81 ± 3.10 cells × 10^5/mL, p = 0.002) or 6 h PMT (mean: 7.19 ± 3.17 cells × 10^5/mL, p = 0.003). The data after 14 days of cultivation were not significantly different. After

28 days of cultivation, both 4 h PMT (mean: 9.30 ± 2.81 cells × 10^5/mL, $p = 0.024$) and 6 h PMT (mean: 10.45 ± 4.20 cells × 10^5/mL, $p = 0.014$) exhibit significantly higher cell numbers than 2 h PMT (mean: 6.51 ± 2.78 cells × 10^5/mL). Confluence data were similar between the groups, with no significant differences. Four and 2 h PMT were the fastest to reach full confluence (median: 8.00 ± 2.25 days) and median: 8.00 ± 3.00 days, respectively), while 6 h PMT needed more time (median: 10.00 ± 4.00 days). The seven-day confluence area was highest at 6 h PMT (median: 92.50% ± 36.25%) compared to 2 h PMT (median: 87.50% ± 38.75%) or 4 h PMT (median: 90.00% ± 60.00%). The rate of unsuccessful cultures was highest for 2 h PMT with 33.33% compared to 4 h PMT with 20.88% and 6 h PMT with 25.25%. Also, the confluence rate was highest at 4 h PMT with 63.19% compared to 2 h and 6 h PMT with 51.85% and 61.11%, respectively.

For morphology, cells were prepared after 2, 4, and 6 h PMT and cultured for 7 (Figure 6A), 14 (Figure 6B), and 28 days (Figure 6C). Light microscopy images were analyzed for the composition of epithelial, mesenchymal, and undivided cells as well as ungrown areas. Between day 7 and day 28, gaps were mainly filled up with mesenchymal cells. After 14 days of cultivation, ungrown areas displayed no differences (0.00% for each condition). After 7 days of cultivation, mesenchymal cells did not show significant differences between the groups. Four-hour PMT showed significantly more epithelial cells (median: 78.33% ± 37.50%) than two-hour PMT (median: 58.34% ± 33.76%, $p < 0.001$) or six-hour PMT (median: 63.33% ± 36.67%, $p = 0.003$), respectively. Six-hour PMT showed significantly more undivided cells (median: 6.67% ± 10.83%) than two-hour PMT (median: 3.33% ± 6.67%, $p < 0.001$) and four-hour PMT (median: 3.33% ± 6.67%, $p < 0.001$). Four-hour PMT showed significantly less ungrown area (median: 1.67% ± 26.67%) than two-hour PMT (median: 18.34% ± 33.34%, $p < 0.001$) or six-hour PMT (median: 8.33% ± 35.84%, $p = 0.042$). Taken together, 4 h PMT can be considered the optimal preparation starting time, as it leads to more epithelial cells and higher cell numbers after one week of cultivation.

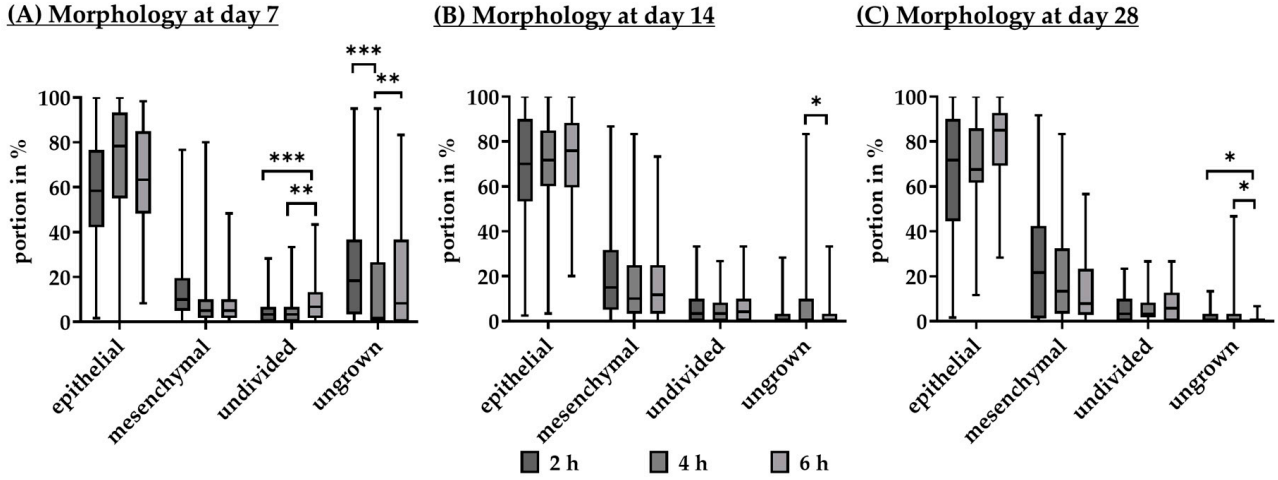

Figure 6. Cell morphology after different post-mortem times. Single-eye retinal pigment epithelium cells were prepared after post-mortem times of 2, 4, and 6 h. The portion of epithelial, mesenchymal, undivided cells, and ungrown areas of each well was determined with light microscopy after 7 ((**A**), $n = 68–159$), 14 ((**B**), $n = 46–83$), and 28 days ((**C**), $n = 22–40$) of cultivation. Data were not parametric; median and interquartile ranges are depicted. Significances were calculated between each group with the Kruskal–Wallis test and Mann–Whitney tests. * $p < 0.05$, ** $p < 0.01$, *** $p < 0.001$, h = hours.

The morphology of actin filaments and cell nuclei was also determined after different PMTs. Cells were prepared after 2, 4, and 6 h PMT and seeded on monomeric collagen I-coated glass slides. Of note, this coating was used as a standard procedure before knowing the results of the coating tests that followed. After 28 days of cultivation, cell nuclei

and actin filaments were stained, and images were taken with fluorescence microscopy. Visual ranking of the quality of the actin cytoskeleton was performed from 0/disturbed (stress fibers and cell gaps) to 5/physiological (proper/circumferential actin) morphology (Figure 7A) by a single observer, which was blinded to the post-mortem time of the cells. Images were evaluated by Fiji (ImageJ2) regarding the number of cell nuclei (Figure 7B), cell nuclei size (Figure 7C), and form factor of cell nuclei (Figure 7D). Example photos for physiological and disturbed actin structure are depicted in Figure 7E. Regarding cell nuclei size and form factor, no significant differences were detected. The quality of the actin cytoskeleton was significantly better after 2 h PMT (median: 4.00 ± 2.50) compared to 4 h (median: 3.50 ± 3.00, $p = 0.017$) and 6 h PMT (median: 3.00 ± 2.50, $p = 0.016$), resembling the physiological RPE situation more closely. Cell nuclei number was significantly higher after 2 h PMT (mean: 499.20 ± 161.08) compared to 4 h (mean: 333.02 ± 168.42, $p < 0.001$) or 6 h PMT (mean: 361.07 ± 114.30, $p < 0.001$). Regarding the actin cytoskeleton, a PMT of 2 h seems to be the optimal condition, which is in contrast to the findings of the former PMT assays. However, the overall ranking differences between 2 h and 4 h PMT are quite small, and only a few cultures survive from a PMT of 2 h, rendering 2 h PMT highly inefficient. Overall, a PMT of 4 h was chosen as the optimal condition regarding cell number, morphology, and success rate. In addition, it also is the most practicable time regarding delivery and lab working hours.

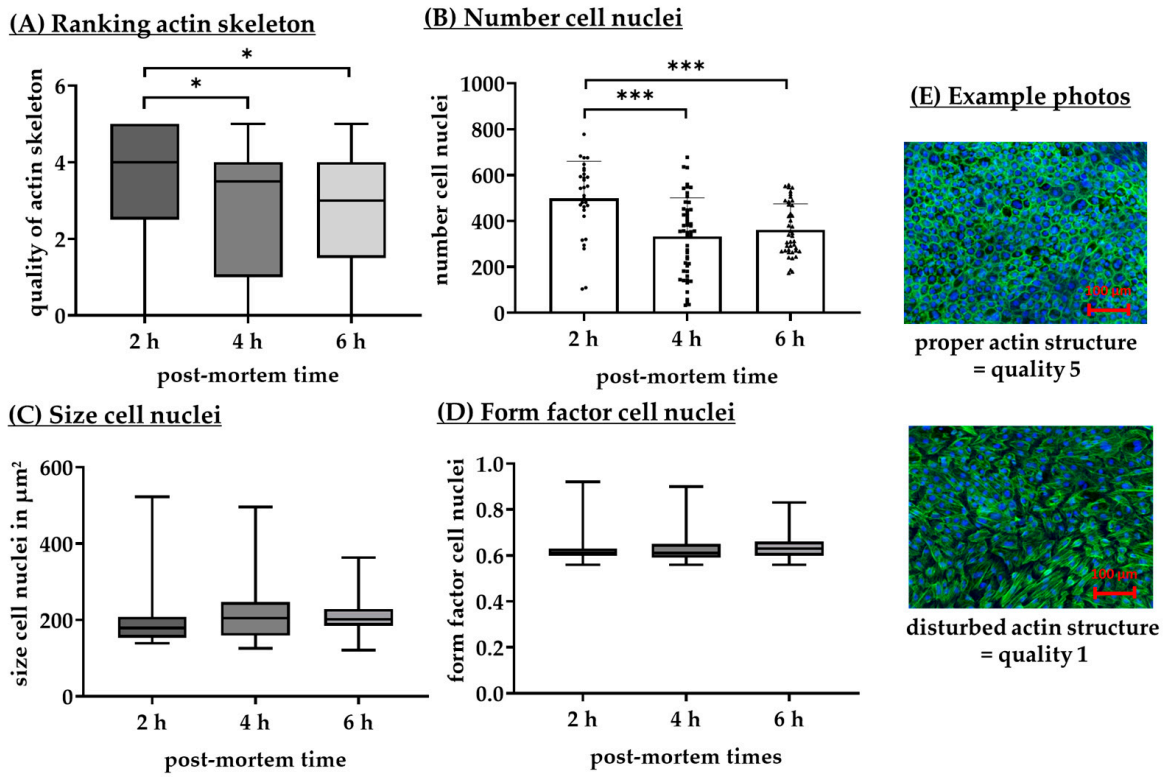

Figure 7. Morphology of actin cytoskeleton and cell nuclei. Single-eye retinal pigment epithelium cells were prepared after post-mortem times of 2, 4, and 6 h and seeded on monomeric collagen I-coated glass slides. After 28 days of cultivation, cell nuclei and actin filaments were stained, and images were taken by fluorescence microscopy. Visual ranking of the quality of the actin cytoskeleton was performed from 0 (disturbed) to 5 (proper) morphology ((**A**), n = 31–51). Images were evaluated by Fiji (ImageJ2) regarding number of cell nuclei ((**B**), n = 30–51), cell nuclei size ((**C**), n = 27–45), and form factor of cell nuclei ((**D**), n = 27–45). Data for (**B**) were parametric; mean and standard deviation are depicted. Significances were calculated between each group with analysis of variance (ANOVA) and Student's t-test. Data for (**A**,**C**,**D**) were not parametric; median and interquartile ranges are depicted. Significances were calculated between each group with the Kruskal–Wallis test

and the Mann–Whitney test. * $p < 0.05$, *** $p < 0.001$, h = hours. Exemplary photos are shown ((**E**), cell nuclei = blue, actin filaments = green, 20× objective, scale bar = 100 µm).

3.2. Coating

3.2.1. Cell Numbers on Different Coatings

Single-eye RPE cells were seeded on different coatings, and the cell numbers were determined. Differences between the cell number on the specific days to the initial seeding cell number were calculated (Figure 8).

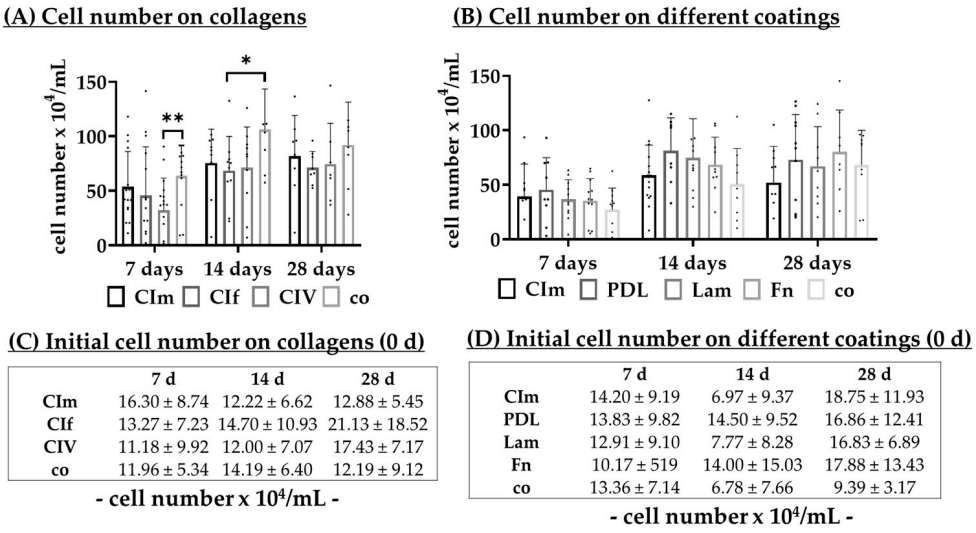

(C) Initial cell number on collagens (0 d)

	7 d	14 d	28 d
CIm	16.30 ± 8.74	12.22 ± 6.62	12.88 ± 5.45
CIf	13.27 ± 7.23	14.70 ± 10.93	21.13 ± 18.52
CIV	11.18 ± 9.92	12.00 ± 7.07	17.43 ± 7.17
co	11.96 ± 5.34	14.19 ± 6.40	12.19 ± 9.12

- cell number x 10^4/mL -

(D) Initial cell number on different coatings (0 d)

	7 d	14 d	28 d
CIm	14.20 ± 9.19	6.97 ± 9.37	18.75 ± 11.93
PDL	13.83 ± 9.82	14.50 ± 9.52	16.86 ± 12.41
Lam	12.91 ± 9.10	7.77 ± 8.28	16.83 ± 6.89
Fn	10.17 ± 519	14.00 ± 15.03	17.88 ± 13.43
co	13.36 ± 7.14	6.78 ± 7.66	9.39 ± 3.17

- cell number x 10^4/mL -

Figure 8. Cell number on different coatings. Before seeding, cells were counted with a trypan blue exclusion assay. ((**A**), n = 7–17) Cells were seeded on monomeric collagen I (CIm), fibrillar collagen I (CIf), collagen IV (CIV), or uncoated wells (co). ((**B**), n = 8–16) Cells were seeded on CIm, Poly-D-Lysine (PDL), laminin (Lam), fibronectin (Fn), or co. Cells were counted again after 7, 14, and 28 days of cultivation, and the difference in the seeding cell number is depicted as cell number × 10^4. The initial cell number mean before seeding is listed for collagen tests ((**C**), n = 7–17) and for coating tests ((**D**), n = 8–16). Data were parametric; mean and standard deviation are shown. Significances were calculated between each group with analysis of variance (ANOVA) and Student's t-test. * $p < 0.05$, ** $p < 0.01$, d = days.

First, different collagens were tested (Figure 8A) with monomeric collagen I (CIm), fibrillar collagen I (CIf), collagen IV (CIV), or uncoated control (co). Numerically, the cell number was highest at all time points when no coating was used (co), followed by CIm. The co condition displayed significantly higher cell numbers than CIV on day 7 (mean: 63.69 ± 28.19 cells × 10^4/mL compared to 32.03 ± 29.68 cells × 10^4/mL, $p = 0.006$). In addition, after 14 days, co displayed significantly higher cell numbers than CIf (mean: 106.13 ± 37.36 cells × 10^4/mL compared to 68.45 ± 31.44 cells × 10^4/mL, $p = 0.030$).

The next step was to investigate the cell number with other coatings (Figure 8B): Poly-D-Lysine (PDL), laminin (Lam), fibronectin (Fn), co, and the most suitable collagen from the collagen testing (CIm). There were no significances or tendencies determined. Numerically, the highest cell number was achieved with PDL on day 7 and day 14, while on day 28, the cell number was highest with fibronectin, followed by PDL.

3.2.2. Confluence on Different Coatings

Single-eye RPE cells were seeded on different coatings and confluency (cell growth area in %) of the well after 7 days, and the day of 95–100% confluency was determined. First, different collagens (CIm, CIf, CIV) compared to the uncoated control (co) were tested. Con-

fluency on day 7 (Figure 9A) was highest if no coating was used (mean: 85.62% ± 24.32%), and this was significantly higher than CIm (mean: 58.66% ± 25.00%, $p < 0.001$), CIf (mean: 39.85% ± 26.65%, $p < 0.001$), or CIV (mean: 48.09% ± 20.34%, $p < 0.001$). CIm displayed a significantly higher confluence on day 7 than CIf ($p = 0.005$). In addition, co reached confluency at the earliest timepoint (Figure 9B, median: day 8.00 ± 2.75), and this was significantly faster than CIm (median: day 13.00 ± 4.00, $p < 0.001$), CIf (median: day 21.00 ± 8.00, $p = 0.004$), or CIV (median: day 15.50 ± 7.70, $p = 0.001$), respectively.

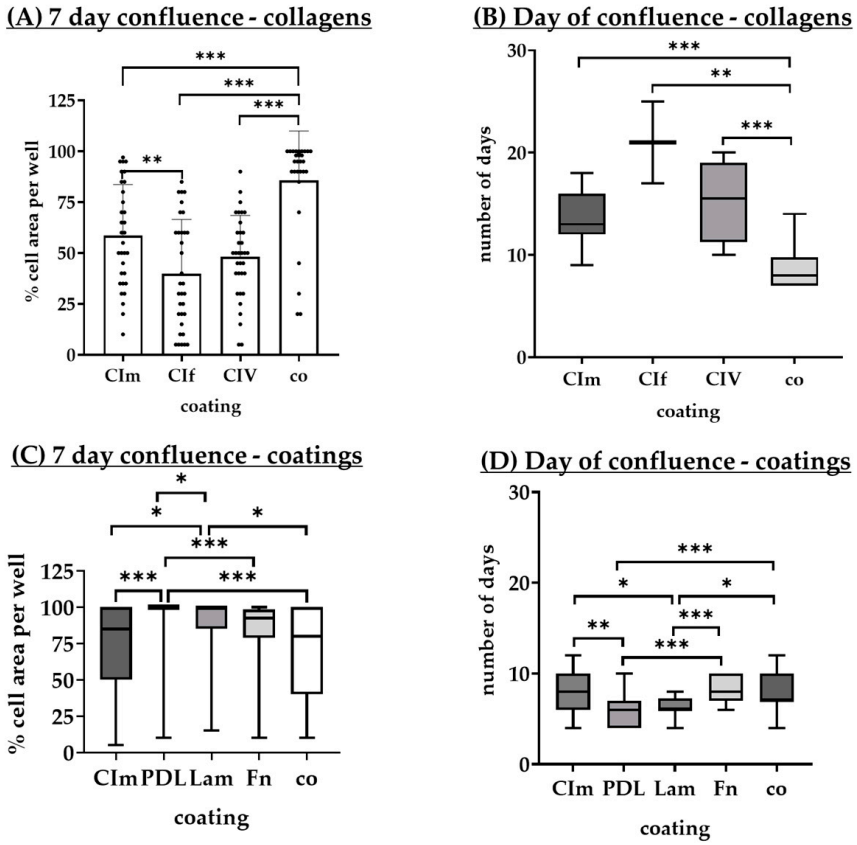

Figure 9. Confluence on different coatings. ((**A**), $n = 29–34$; (**B**), $n = 2–20$) Single-eye retinal pigment epithelium cells were seeded on monomeric collagen I (CIm), fibrillar collagen I (CIf), collagen IV (CIV), or uncoated wells (co). ((**C**), $n = 28–36$; (**D**), $n = 17–27$) Cells were seeded on CIm, Poly-D-Lysine (PDL), laminin (Lam), fibronectin (Fn), or co. Confluence as a cell growth area in % of the well was determined with light microscopy after 7 days of cultivation (**A**,**C**), and the day of 95–100% confluency was determined (**B**,**D**). For (**A**), data were parametric; mean and standard deviation are shown. Significances were calculated between each group with analysis of variance (ANOVA) and Student's *t*-test. For (**B**–**D**), data were not parametric; median and interquartile ranges are depicted. Significances were calculated between each group with the Kruskal–Wallis test and the Mann–Whitney test. * $p < 0.05$, ** $p < 0.01$, *** $p < 0.001$.

The next step was to investigate the confluence of the coatings' PDL, Lam, and Fn, together with CIm and co. Regarding 7-day confluency (Figure 9C), PDL reached complete confluency (median: 100.00% ± 0.00%), which was significantly different to CIm (median: 85.00% ± 50.00%, $p < 0.001$), Lam (median: 100.00% ± 15.00%, $p < 0.030$), Fn (median: 92.50% ± 19.70%, $p < 0.001$), or co (median: 80.00% ± 60.00%, $p < 0.001$), respectively. Lam also exhibited full confluency on day 7, and this was significantly higher than CIm ($p = 0.020$) and co ($p = 0.030$). Concerning the day of full confluence (Figure 9D), PDL was the first to reach it (median: day 6.00 ± 3.00). This effect was significantly different compared to CIm (median: day 8.00 ± 4.00, $p = 0.007$), Fn (median: day 8.00 ± 3.00,

$p < 0.001$), or co (median: day 7.00 ± 3.00, $p < 0.002$), respectively. The second best coating regarding the day of confluence was Lam (median: day 6.00 ± 1.25). This was significantly better than CIm ($p = 0.030$), Fn ($p < 0.001$) or co ($p = 0.020$), respectively. Overall, confluence on day 7 and time to reach full confluence was optimal with PDL.

3.2.3. Morphology on Different Coatings

Single-eye RPE cells were seeded on different coatings for 7, 14, and 28 days, and light microscopy images of different areas of the well were analyzed for composition of epithelial, mesenchymal, and undivided cells, as well as ungrown areas (% well area).

First, different collagens (CIm, CIf, CIV) were tested and compared to the uncoated control (co) (Figure 10A–C). After 7 days of cultivation (Figure 10A), co contained most epithelial cells (median: 80.00% ± 45%), which was significantly higher than CIf (median: 12.50% ± 58.80%, $p < 0.001$) or CIV (median: 40.00% ± 50.00%, $p < 0.001$). Also, CIm (median: 55.00% ± 60%) contained more epithelial cells than CIf ($p = 0.004$) or CIV ($p = 0.040$). Ungrown areas were the least likely to be found with co (median: 2.50% ± 32.50%). CIf (median: 65.00% ± 73.75%, $p = 0.003$) and CIV (median: 15.00% ± 57.50%, $p = 0.030$) showed significantly more gaps in the cell layer compared to co. After 14 days of cultivation (Figure 9B), again, co contained most epithelial cells (median: 92.50% ± 15.00%), which was significantly higher than CIf (median: 45.00% ± 47.50%, $p < 0.001$), CIV (median: 65.00% ± 65.00%, $p < 0.001$), or CIm (median: 80.00% ± 20.00%, $p = 0.020$). CIm had significantly more epithelial cells than CIf ($p < 0.001$). Accordingly, co had the fewest mesenchymal cells (median: 7.50% ± 18.80%), which was significantly lower than CIf (median: 47.50% ± 51.20%, $p < 0.001$), CIV (median: 30.00% ± 60.00%, $p = 0.001$), or CIm (median: 12.50% ± 23.75%, $p = 0.040$). CIm had significantly fewer mesenchymal cells than CIf ($p < 0.001$). After 28 days of cultivation (Figure 10C), all conditions reached full confluency (no ungrown areas, all medians: 0.00% ± 0.00%). Undivided cells were quite few, with CIf showing the most (CIm median: 0.00% ± 3.75%; CIf median: 5.00% ± 5.00%; CIV median: 0.00% ± 5.00%; co median: 0.00% ± 5.00%). Most epithelial and the least number of mesenchymal cells were achieved on uncoated wells (median: 90.00% ± 13.70% and 5.00% ± 13.80%, respectively), followed by CIm (median: 85.00% ± 33.80% and 15.00% ± 38.75%, respectively). Co condition showed significantly more epithelial cells than CIm ($p = 0.001$), CIf (median: 22.50% ± 61.30%, $p < 0.001$), or CIV (median: 70.00% ± 72.50%, $p = 0.001$). Also, CIm contained more epithelial cells than CIf ($p < 0.001$). Correspondingly, co contained significantly fewer mesenchymal cells than CIm ($p = 0.030$), CIf (median: 70.00% ± 73.70%, $p < 0.001$), or CIV (median: 30.00% ± 77.50%, $p < 0.001$). Additionally, CIm had significantly fewer mesenchymal cells than CIf ($p = 0.002$).

In addition, different coatings (PDL, Lam, Fn) were tested and compared to CIm and co (Figure 10D–F). After 7 days of cultivation (Figure 10D), CIm (median: 67.50% ± 60.00%) showed significantly fewer epithelial cells than PDL (median: 85.00% ± 35.00%, $p = 0.004$), Lam (median: 85.00% ± 20.00%, $p < 0.001$), or co (median: 80.00% ± 40.00%, $p = 0.005$). Fn (median: 65.00% ± 50.00%) also contained fewer epithelial cells than Lam ($p = 0.009$) or co ($p = 0.040$). CIm (median: 15.00% ± 25.00%) displayed significantly more mesenchymal cells than PDL (median: 5.00% ± 20.00%, $p = 0.020$), Lam (median: 5.00% ± 15.00%, $p = 0.030$), or co (median: 10.00% ± 20.00%, $p = 0.049$). Fn (median: 10.00% ± 45.00%) contained significantly more mesenchymal cells than PDL ($p = 0.020$), Lam ($p = 0.040$), or co ($p = 0.049$). After 14 days of cultivation (Figure 10E), PDL (median: 95.50% ± 12.50%) showed significantly more epithelial cells than CIm (median: 80.00% ± 42.50%, $p < 0.001$) or Fn (median: 80.00% ± 25.00%, $p = 0.030$). Lam (median: 90.00% ± 25.00%) contained more epithelial cells than CIm ($p = 0.020$). PDL (median: 0.00% ± 10.00%) had fewer mesenchymal cells than CIm (median: 15.00% ± 31.30%, $p < 0.001$), Fn (median: 15.00% ± 25.00%,

$p = 0.004$), or co (median: 10.00% ± 30.00%, $p = 0.007$). Also, Lam (median: 0.00% ± 10.00%) had fewer mesenchymal cells than CIm ($p = 0.007$). After 28 days of cultivation (Figure 10F), all conditions reached full confluency. Undivided cells were almost undetectable and not significantly different for any tested condition. Most epithelial and the least number of mesenchymal cells were achieved on PDL-coated wells (median: 95.00% ± 10.00% and 0.00% ± 5.00%, respectively), followed by Lam-coated wells (median: 90.00% ± 20.00% and 0.00% ± 10.00%, respectively). PDL showed significantly more epithelial cells than CIm (median: 75.00% ± 48.80%, $p < 0.001$) and Fn (median: 80.00% ± 27.50%, $p = 0.030$). Also, Lam showed more epithelial cells than CIm ($p = 0.02$). The co condition was similar to Lam (mean: 90.00% ± 35.00%). In accordance, PDL displayed significantly fewer mesenchymal cells than CIm (mean: 10.00% ± 42.50%, $p < 0.001$), Fn (median: 10.00% ± 25.00%, $p = 0.007$), or co (median: 5.00% ± 35.00%, $p = 0.010$). Additionally, Lam had significantly fewer mesenchymal cells than CIm ($p = 0.020$). Overall, RPE on PDL-coated wells showed the highest proportion of epithelial cells.

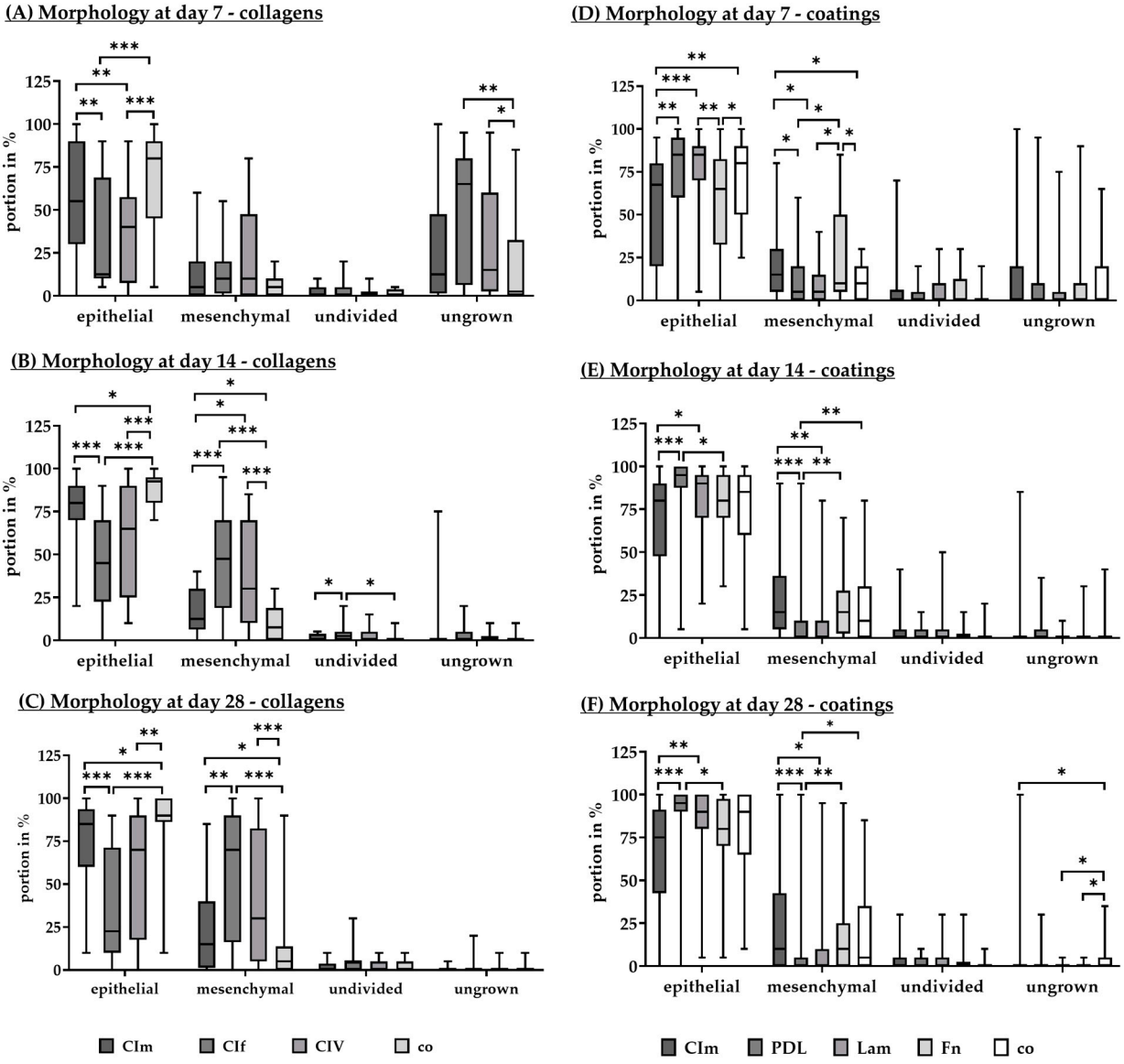

Figure 10. Cell morphology on different collagens and other coatings. Single-eye retinal pigment epithelium cells were seeded on monomeric collagen I (CIm), fibrillar collagen I (CIf), collagen IV (CIV), or uncoated wells (co) ((**A**), $n = 21–24$; (**B**), $n = 21–24$; (**C**), $n = 21–24$). After determining optimal collagen, coatings CIm, Poly-D-Lysine (PDL), laminin (Lam), fibronectin (Fn), and uncoated wells (co)

were tested ((**D**), n = 21–33; (**E**), n = 21–33; (**F**), n = 21–33). The portion of epithelial, mesenchymal, undivided cells, and ungrown areas of each well was determined with light microscopy after 7 ((**A**) + (**D**)), 14 ((**B**) + (**E**)), and 28 days ((**C**) + (**F**)) of cultivation. Data were not parametric; median and interquartile ranges are shown. Significances were calculated between each group with the Kruskal–Wallis test and the Mann–Whitney test. * $p < 0.05$, ** $p < 0.01$, *** $p < 0.001$.

3.2.4. Success Rates on Different Coatings

For RPE wells used for the experiments of collagen pretesting, survival rates and confluence rates were determined for all cultures combined. Of all 141 seeded wells, 128 were viable (please refer to Section 3.1.2 for the definition of success rates) until the day of the experiment, which equals a survival rate of 90.78%. From these 128 wells, only 27.34% reached 95–100% confluence, which is quite low and strongly indicates that collagen coating is suboptimal. These data were also assessed for the different collagen coatings (CIm, CIf, and CIV) compared to uncoated co after 7, 14, and 28 days (Table 3). In contrast to co, none of the collagen coatings reached confluence after day 7. For all time points, co showed the highest confluence rate, followed by CIm. The survival rate was the highest with the CIV coating (97.14%). Overall, co was better suited than any collagen coating tested.

Table 3. Success rates depending on the collagen type. Confluence and survival rates are listed according to the specific collagen coating with monomeric collagen I (CIm), fibrillar collagen I (CIf), collagen IV (CIV), or uncoated wells (co), as well as days of cultivation (d). The highest rates are marked. Numeric and percentage rates of success to the overall number of cultures are depicted.

Success Rates				
Coatings	**co**	**CIm**	**CIV**	**CIf**
7 d confluence % (living wells)	**9/29** **31.03%**	0/32 0.00%	0/34 0.00%	0/33 0.00%
14 d confluence % (living wells)	**20/29** **68.97%**	5/32 15.63%	1/34 2.94%	0/33 0.00%
28 d confluence % (living wells)	**20/29** **68.97%**	9/32 28.13%	4/34 11.76%	2/33 6.06%
7 d confluence % (total wells)	**9/34** **26.47%**	0/36 0.00%	0/35 0.00%	0/36 0.00%
14 d confluence % (total wells)	**20/34** **58.82%**	5/36 13.89%	1/35 2.86%	0/36 0.00%
28 d confluence % (total wells)	**20/34** **58.82%**	9/36 25.00%	4/35 11.43%	2/36 5.56%
Survival (living wells/total wells)	29/34 85.29%	32/36 88.89%	**34/35** **97.14%**	33/36 91.67%

Also, for the follow-up experiments with coating substances CIm, PDL, Lam, Fn, and co, success rates for survival and confluence were determined for all cultures combined. Altogether, the survival rate was 96.25%, and the confluence rate was 69.48%. Stratified for the coating (Table 4), the data reveal that PDL shows the highest confluence rates, reaching 90% and more after 14 and 28 days, followed by Lam. Conversely, survival rates of CIm and Fn were at a maximum of 100% (Table 4).

Table 4. Success rates depending on the coating. Confluence and survival rates are listed according to the specific coating with monomeric collagen I (CIm), Poly-D-Lysine (PDL), laminin (Lam), fibronectin (Fn), or uncoated wells (co), as well as days of cultivation (d). The highest rates are marked. Numeric and percentage rates of success to the overall number of cultures are depicted.

Success Rates					
Coatings	**CIm**	**PDL**	**Lam**	**Fn**	**co**
7 d confluence % (living wells)	10/36 27.78%	**23/28** **82.14%**	17/31 54.84%	7/30 23.33%	9/29 31.03%
14 d confluence % (living wells)	21/36 58.33%	**27/28** **96.43%**	22/31 70.97%	20/30 66.67%	17/29 58.62%
28 d confluence % (living wells)	21/36 58.33%	**27/28** **96.43%**	22/31 70.97%	20/30 66.67%	17/29 58.62%
7 d confluence % (total wells)	10/36 27.78%	**23/30** **76.67%**	17/32 53.13%	7/30 23.33%	9/32 28.13%
14 d confluence % (total wells)	21/36 58.33%	**27/30** **90.00%**	22/32 68.75%	20/30 66.67%	17/32 53.13%
28 d confluence % (total wells)	21/36 58.33%	**27/30** **90.00%**	22/32 68.75%	20/30 66.67%	17/32 53.13%
Survival (living wells/total wells)	**36/36** **100.00%**	28/30 93.33%	31/32 96.88%	**30/30** **100.00%**	29/32 90.63%

3.2.5. Growth Factor Secretion on Different Coatings

To assess the secretion of VEGF-A of single-eye RPE cells cultured on different coatings (CIm, PDL, Lam, Fn, and co), supernatants were collected for 4 h on days 7, 14, and 28 after preparation and analysis with VEGF ELISA (Figure 11). Secreted VEGF ranged from 735.33 ± 164.03 pg/mL (PDL, 28 days) and 1109.33 ± 276.78 pg/mL (co, 28 days), which was in the normal range of the VEGF secretion of primary porcine mix culture RPE [39]. On day 7 and day 14, no significant differences between coatings were detected. On day 28 of cultivation, Lam showed significantly higher VEGF-A concentrations than PDL (mean: 1038.50 ± 248.47 pg/mL compared to 735.33 ± 164.03 pg/mL, $p = 0.009$), Fn displayed significantly lower concentrations than Lam (mean: 738.00 ± 161.08 pg/mL compared to 1038.50 ± 248.47 pg/mL, $p = 0.020$), and co showed significantly higher concentrations than Fn (mean: 1109.33 ± 276.78 pg/mL compared to 738.00 ± 161.08 pg/mL, $p = 0.010$) or PDL (mean: 1109.33 ± 276.78 pg/mL compared to 735.33 ± 164.03 pg/mL, $p = 0.006$). It is of interest that the previously determined most suitable coating, PDL, displayed the lowest VEGF secretion.

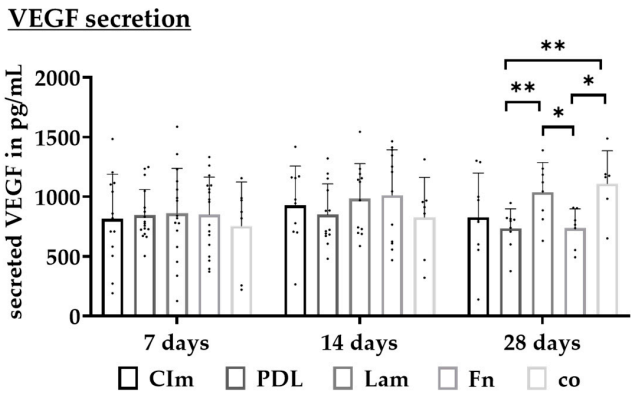

Figure 11. VEGF secretion on different coatings. Single-eye retinal pigment epithelium cells were seeded on monomeric collagen I (CIm), Poly-D-Lysine (PDL), laminin (Lam), fibronectin (Fn), or uncoated wells

(co). The supernatant was collected for 24 h after 7, 14, and 28 days of cultivation and analyzed in ELISA for vascular endothelial growth factor A (VEGF-A). n = 6–17. Data were parametric; mean and standard deviation are shown. Significances were calculated between each group with analysis of variance (ANOVA) and Student's t-test. * $p < 0.05$, ** $p < 0.01$, d = days.

3.2.6. Protein Expression on Different Coatings

RPE65 and CLDN19 are physiologically expressed RPE proteins, indicating differentiation and tight junction formation [40]. RPE cells were seeded on CIm, PDL, Lam, Fn, or on uncoated wells (co), and protein expression of RPE65 and CLDN19 was investigated with Western blotting (Figure 12 with example images) after 14 and 28 days of cultivation.

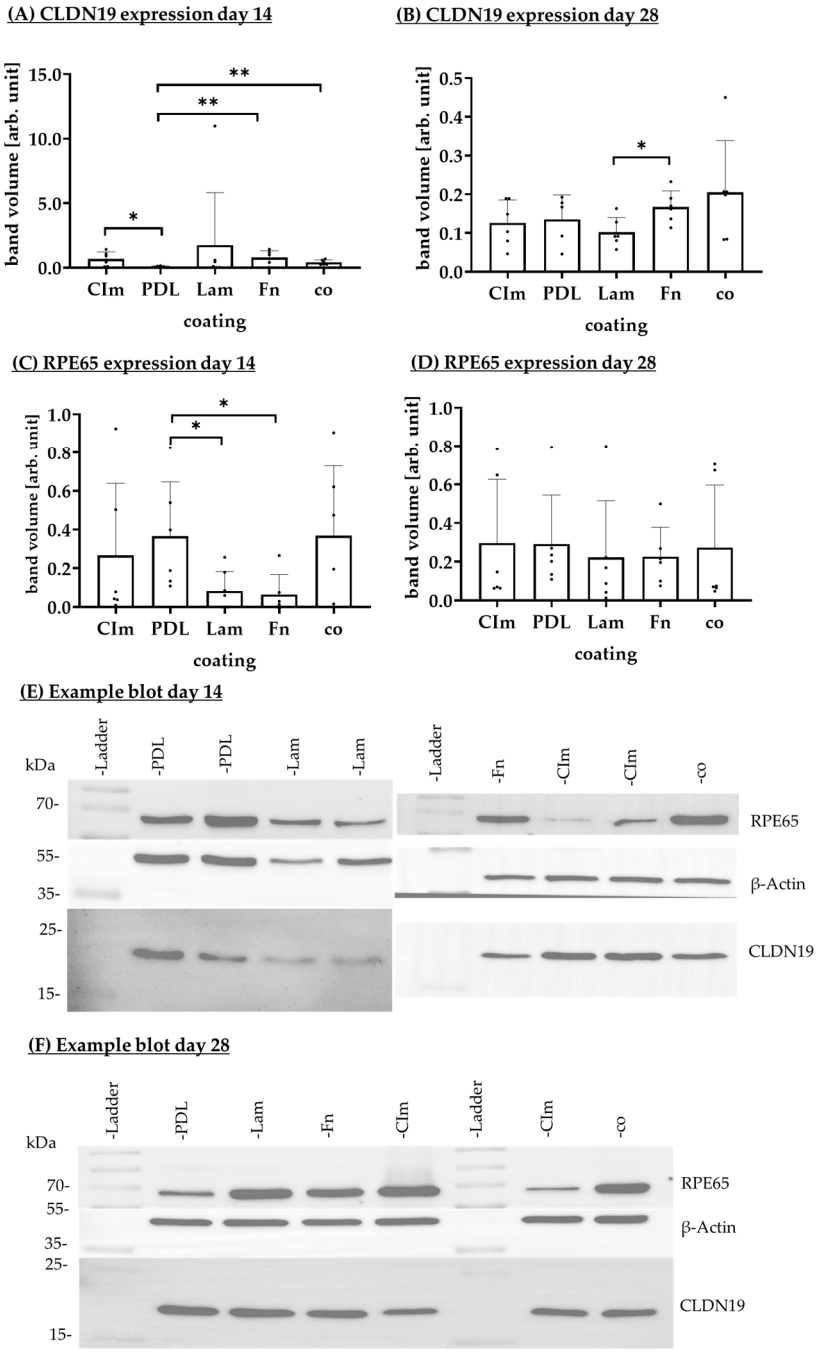

Figure 12. RPE65 and CLDN19 expression on different coatings. Single-eye retinal pigment epithelium cells were seeded on monomeric collagen I (CIm), Poly-D-Lysine (PDL), laminin (Lam), fibronectin (Fn),

or uncoated wells (co). Lysates were made after 14 ((**A**), n = 6–7; (**C**), n = 6–7) and 28 days ((**B**), n = 5–6; (**D**), n = 6) of cultivation and analyzed with Western blotting for claudin-19 (CLDN19, (**A**,**B**) and retinal pigment epithelium-specific 65 kDa protein (RPE65, (**C**,**D**). Data were parametric; mean of band volumes normalized to β-actin expression and standard deviation are depicted. Significances were calculated between each group with analysis of variance (ANOVA) and Student's t-test. * $p < 0.05$, ** $p < 0.01$. (**E**,**F**) Exemplary blots for 14 and 28 days are depicted.

Regarding CLDN19 expression on day 14 (Figure 12A), Lam showed the highest values with 1.74 ± 4.08 [arb. unit] and PDL showed the lowest values with 0.08 ± 0.05 [arb. unit]. Fn (mean: 0.79 ± 0.52 [arb. unit], $p = 0.008$) and co (mean: 0.42 ± 0.19 [arb. unit], $p = 0.002$) were significantly higher than PDL. CIm also exhibited higher CLDN19 expression than PDL (mean: 0.67 ± 0.55 [arb. unit], $p = 0.025$). Concerning CLDN19 expression on day 28 (Figure 12B), co showed the highest expression with 0.20 ± 0.13 [arb. unit] and Lam showed the lowest expression with 0.10 ± 0.04 [arb. unit]. Fn showed significantly higher values than Lam (mean: 0.17 ± 0.04 [arb. unit], $p = 0.017$).

Regarding RPE65 expression on day 14 (Figure 12C), both co and PDL showed equally high expressions with 0.37 ± 0.36 [arb. unit] and 0.37 ± 0.28 [arb. unit], respectively. Fn displayed the lowest values with 0.06 ± 0.10 [arb. unit]. PDL was significantly higher than Lam (mean: 0.08 ± 0.10 [arb. unit], $p = 0.030$) and Fn ($p = 0.033$). After 28 days of cultivation (Figure 12D), no significant differences were determined, but PDL showed the highest values with 0.29 ± 0.25 [arb. unit] and Lam showed the lowest values with 0.22 ± 0.29 [arb. unit]. Overall, PDL showed the highest RPE65 expression, indicating a higher level of differentiation. After 14 days of cultivation, the PDL coating showed little CLDN19 expression, but after 28 days, expression levels were comparable to the other coatings.

3.2.7. Cell Parameters on Different Coatings

To further investigate the differentiation and formation of single-eye RPE cells on different coatings, RPE cells were assessed for tight junction/cell border formation and other cellular parameters (see below). RPE cells were seeded on CIm, PDL, Lam, or Fn-coated glass coverslips (compared to uncoated slips, co) for 28 days. Cells were labeled for cell nuclei (blue) and tight junction protein CLDN19 (orange), and fluorescence images were taken.

First, a visual ranking of the quality of the cell borders (orange channel CLDN19) was conducted (Figure 13) by a single researcher, blinded to culture conditions. The ranking is from 0 for disturbed cell formation to 5 for differentiated and honeycomb-like RPE. The highest ranking was achieved by the Lam coating and co (median: 4.00 ± 1.50 and 4.00 ± 1.00, respectively). CIm, PDL, and Fn exhibited similar quality (median: 3.50 ± 1.00). Lam showed significantly better tight junction formation than Fn ($p = 0.040$) or PDL ($p = 0.010$). Co had a significantly higher ranking than CIm ($p = 0.009$), PDL ($p < 0.001$), or Fn ($p = 0.001$).

PDL seemed not to be suitable for coverslip coating. RPE cells on PDL-coated glass coverslips were affected by the staining procedure, disturbing the ranking quality of the cell border formation or even leading to cell detachment (Figure 13C).

The highest quality images of the cells (ranking 4 to 5) were used to determine morphological parameters and calculate optimal parameters for porcine primary RPE (Table 5) with CellProfiler software. Out of 341 images, 42.82% could not be evaluated by the software. For evaluation in CellProfiler, clearly visible cell borders and cell nuclei in a honeycomb structure were needed. Based on the evaluation of the analyzable images, the mean cell number of the images of a porcine single-eye RPE culture was 472.31 ± 97.61. Cells had a

size of 324.25 ± 76.15 µm^2, a perimeter of 76.02 ± 8.04 µm^2, an eccentricity of 0.63 ± 0.01, a form factor of 0.68 ± 0.02 (which equals hexagonal shape), and a radius of 2.93 ± 0.32 µm. If data are differentiated based on the coating condition (Table 6), the PDL coating displayed the closest values to the standard calculation for cell area with 303.10 µm^2 and a perimeter of 75.28 µm. Eccentricity and form factor were nearly identical. Cell number and radius were closest to the standard values for no coating (co).

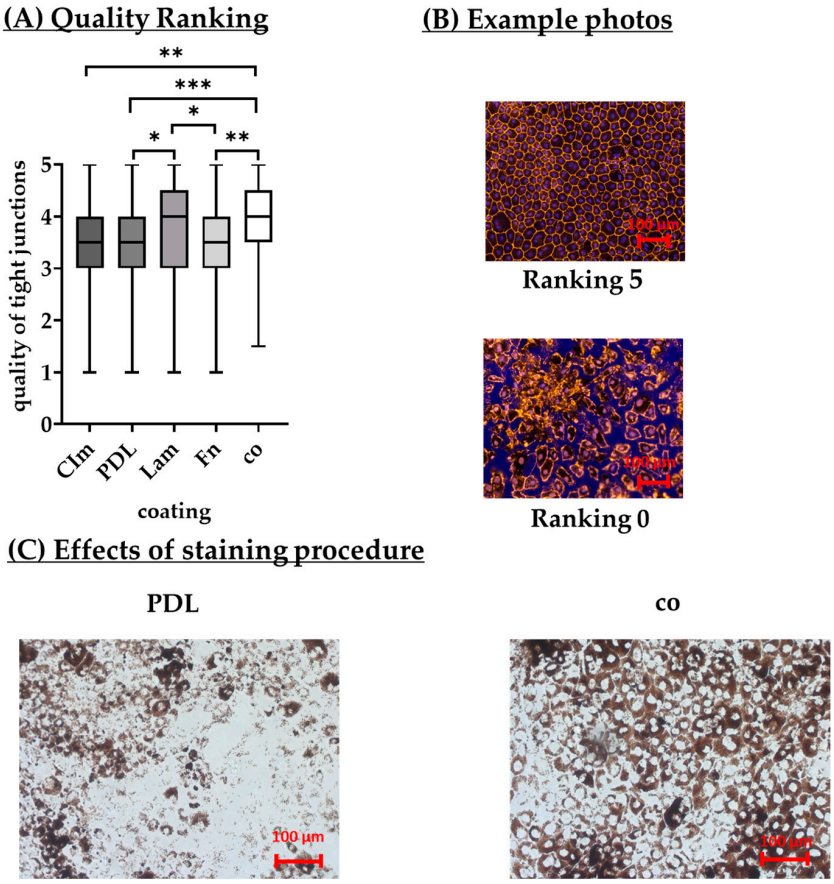

Figure 13. Formation of tight junctions. Single-eye retinal pigment epithelium cells were seeded on monomeric collagen I (CIm), Poly-D-Lysine (PDL), laminin (Lam), fibronectin (Fn), or uncoated wells (co). Tight junction protein claudin-19 was labeled and detected by fluorescence microscopy after 28 days of cultivation. n = 53–89. (**A**) The quality of the cell formation was visually ranked from 0 (disturbed) to 5 (honeycomb structure). Data were not parametric; median and interquartile ranges are shown. Significances were calculated between each group with the Kruskal–Wallis test and the Mann–Whitney test. * $p < 0.05$, ** $p < 0.01$, *** $p < 0.001$. (**B**) Exemplary images are shown for ranking 0 and ranking 5 (20× objective, scale bar = 100 µm). (**C**) Exemplary photos of PDL-coated glass coverslips and uncoated glass coverslips (co) after the staining procedure for immunofluorescence imaging (20× objective, light microscopy, scale bar = 100 µm) are shown. Single-eye retinal pigment epithelium cells were cultivated on these slips for 28 days. Cells on the PDL coating were affected by the staining procedure.

Table 5. Standard values of differentiated porcine single-eye retinal pigment epithelium cells. Single-eye retinal pigment epithelium cells were seeded on glass coverslips and stained for cell nuclei and tight junction protein claudin-19 after 28 days of cultivation. Fluorescence images were taken and evaluated with CellProfiler. n = 54.

	Cell Number	Area (µm^2)	Perimeter (µm)	Eccentricity	Form Factor	Radius (µm)
Mean	472.31	324.25	76.02	0.63	0.68	2.93
Standard deviation	97.61	76.15	8.04	0.01	0.02	0.32

Table 6. Cell parameters depending on coating. Porcine single-eye retinal pigment epithelium cells were seeded on monomeric collagen I (CIm), Poly-D-Lysine (PDL), laminin (Lam), fibronectin (Fn), or uncoated glass coverslips (co) and stained for cell nuclei and tight junction protein claudin-19 after 28 days of cultivation. Fluorescence images were taken and evaluated with CellProfiler. Green marked data are closest and yellow marked data are second closest to the calculated standard values in Table 3. n = 12–43.

Coating	Cell Number	Area (µm^2)	Perimeter (µm)	Eccentricity	Form Factor	Radius (µm)
CIm	444.97	357.55	80.11	0.64	0.67	3.02
PDL	499.23	303.10	75.28	0.65	0.66	2.77
Lam	517.65	295.40	74.41	0.64	0.66	2.74
Fn	416.17	366.34	80.97	0.64	0.67	3.07
co	463.64	348.50	80.40	0.65	0.66	2.95

The results of this section indicate that cells should be seeded on uncoated glass for staining assays.

3.3. Serum Content

3.3.1. Cell Numbers with Different Serum Content

Single-eye RPE cells were cultivated in different serum conditions, and cell number was determined before seeding and after cultivation periods of 7, 14, and 28 days with a trypan blue exclusion assay. Differences between cell count on the respective day of culture to the initial seeding cell number were calculated (Figure 14).

(A) Cell number difference

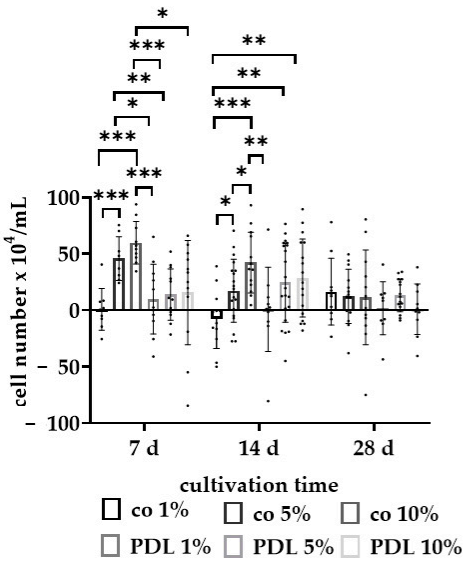

(B) Initial cell number (0 d)

	7 d	14 d	28 d
co 1%	44.54 ± 27.92	21.79 ± 18.55	44.00 ± 11.47
co 5%	29.65 ± 30.05	18.66 ± 11.67	15.19 ± 11.85
co 10%	36.07 ± 26.65	18.38 ± 11.70	9.13 ± 7.83
PDL 1%	37.36 ± 27.38	19.33 ± 20.01	12.50 ± 10.01
PDL 5%	32.61 ± 13.02	18.68 ± 15.04	14.95 ± 17.01
PDL 10%	49.54 ± 30.20	19.33 ± 11.38	12.04 ± 14.25

– cell number x 10^4/mL –

Figure 14. Cell number in different serum conditions. Before seeding single-eye retinal pigment epithelium, cell number was assessed with a trypan blue exclusion assay. Cells were seeded on Poly-D-Lysine (PDL) or uncoated wells (co) and cultivated in medium with 1%, 5%, or 10% serum. Cells were counted again after 7, 14, and 28 days of cultivation, and the differences in the seeding cell are depicted as cell number × 10^4/mL ((**A**), n = 8–21). The initial cell number mean before seeding is listed ((**B**), n = 8–21). Data were parametric; mean and standard deviation are shown. Significances were calculated between each group with analysis of variance (ANOVA) and Student's t-test. * $p < 0.05$, ** $p < 0.01$, *** $p < 0.001$.

On day 28, no significant differences were determined. On day 14, only co 1% displayed a negative cell growth of −7.71 ± 25.12 cells × 10^4/mL. After 7 days, co

10% (59.73 ± 17.85 cells × 10^4/mL) was significantly higher than co 1% (0.73 ± 17.35 cells × 10^4/mL, $p < 0.001$), PDL 1% (9.82 ± 29.48 cells × 10^4/mL, $p = 0.010$), PDL 5% (13.92 ± 21.79 cells × 10^4/mL, $p < 0.001$), or PDL 10% (15.63 ± 44.25 cells × 10^4/mL, $p = 0.010$). Co 5% (46.69 ± 18.17 cells × 10^4/mL) was significantly higher than co 1% ($p < 0.001$), PDL 1% ($p = 0.010$), or PDL 5% ($p = 0.005$). After 14 days of cultivation, co 1% showed significantly fewer cells than co 5% (17.30 ± 27.12 cells × 10^4/mL, $p = 0.019$), co 10% (42.15 ± 25.90 cells × 10^4/mL, $p < 0.001$), PDL 5% (24.50 ± 34.39 cells × 10^4/mL, $p = 0.001$), or PDL 10% (28.47 ± 33.50 cells × 10^4/mL, $p = 0.005$), respectively. Co 10% showed a significantly higher cell number than co 5% ($p = 0.018$) or PDL 1% (0.80 ± 35.41 cells × 10^4/mL, $p = 0.006$). Overall, in the first 2 weeks of cultivation, cells without coating and with a higher serum ratio show an increased cell number, but this difference is lost after 4 weeks of cultivation.

3.3.2. Confluence with Different Serum Content

Single-eye RPE cells were seeded on PDL or uncoated wells (co) with different serum content of medium (1%, 5%, and 10%), and confluency (cell growth area in % of the well) after 7 days as well as the day of 95–100% confluency was determined in light microscopy.

Confluency on day 7 (Figure 15A) was the highest with PDL 10% (median: 100.00% ± 15.00%), and the lowest with co 1% (median: 80.00% ± 47.50%). PDL 10% was significantly higher than co 10% (median: 90.00% ± 30.00%, $p = 0.019$), co 5% (median: 85.00% ± 40.00%, $p = 0.004$), co 1% ($p = 0.002$), or PDL 1% (median: 90.00% ± 45.00%, $p = 0.005$), respectively. PDL 5% (median: 95.00% ± 22.50%) showed higher confluence on day 7 than co 1% ($p = 0.034$).

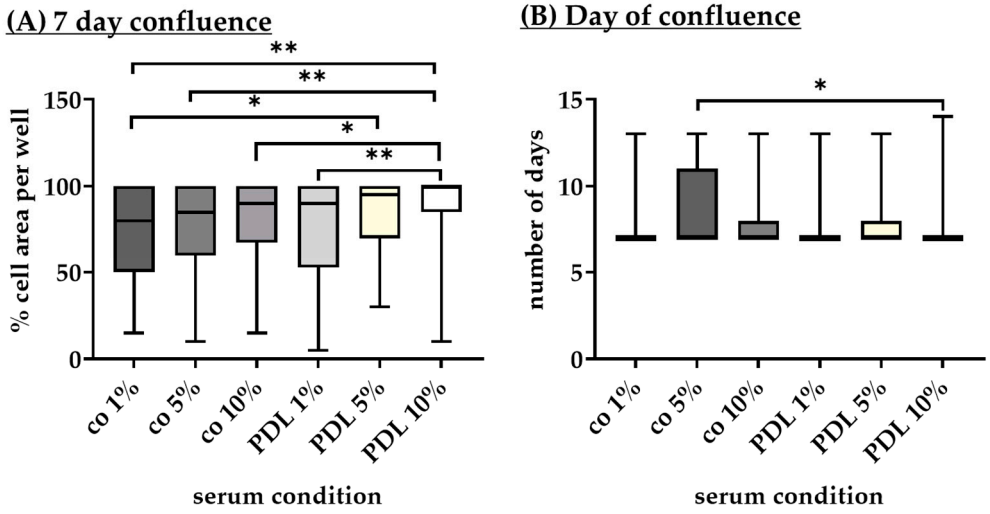

Figure 15. Confluence in different serum conditions. Single-eye retinal pigment epithelium cells were seeded on Poly-D-Lysine (PDL) or uncoated wells (co) and cultivated in medium with 1%, 5%, or 10% serum. Confluence as a cell growth area in % of the well after 7 days of cultivation ((**A**), $n = 43–51$) and the day of 95–100% confluency was determined ((**B**), $n = 16–27$). Data were not parametric; median and interquartile ranges are depicted. Significances were calculated between each group with the Kruskal–Wallis test and the Mann–Whitney test. * $p < 0.05$, ** $p < 0.001$.

The median of the day of full confluence (Figure 15B) was the same for all conditions (day 7.00). The only variation was in the interquartile range, which was the highest for co 5% with 3.75 days and significantly different from PDL 10% with an interquartile range of 0.00 ($p = 0.038$).

The data show that in cultivation periods of 7 and 14 days, cell number and confluency increase with increasing serum content. The faster division of the cells is highly likely due

to the growth factor provided by the serum. After 28 days, however, cell number and confluence are no longer dependent on serum content.

3.3.3. Morphology with Different Serum Content

The morphology of cells grown in a medium with different serum content (1%, 5%, 10%) was analyzed by light microscopy after 7 (Figure 16A), 14 (Figure 16B), and 28 days (Figure 16C).

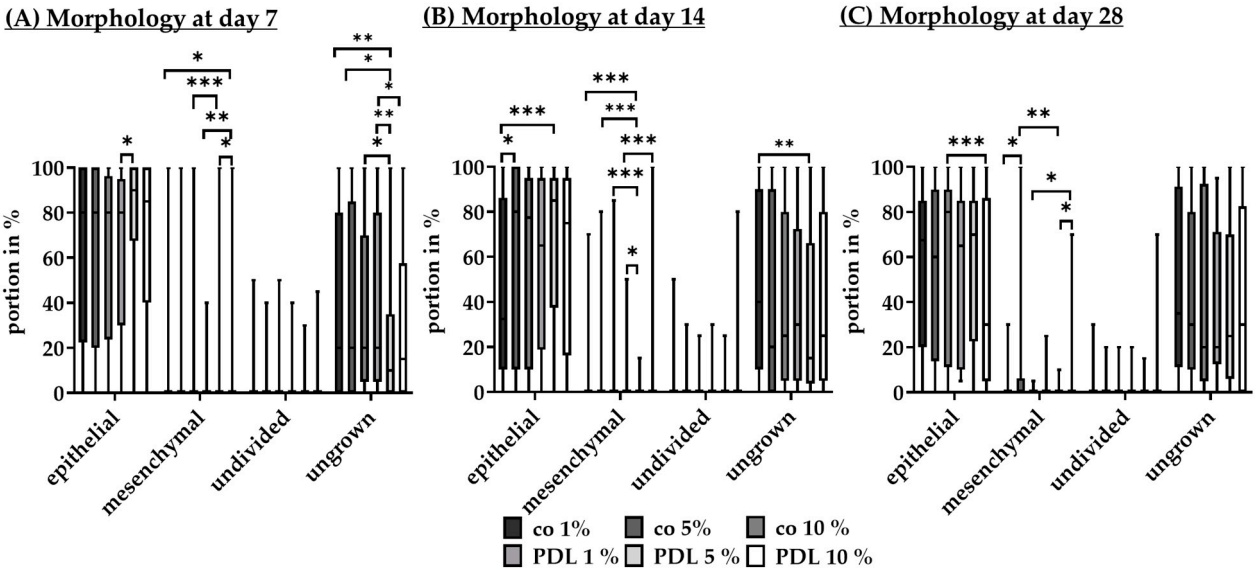

Figure 16. Cell morphology in different serum conditions. Single-eye retinal pigment epithelium cells were seeded on Poly-D-Lysine (PDL) or uncoated wells (co) and cultivated in medium with 1%, 5%, or 10% serum. The portion of epithelial, mesenchymal, undivided cells, and ungrown areas of each well was determined with light microscopy after 7 ((**A**), n = 126–153), 14 ((**B**), n = 96–120), and 28 days ((**C**), n = 33–51) of cultivation. Data were not parametric; median and interquartile ranges are shown. Significances were calculated between each group with the Kruskal–Wallis test and the Mann–Whitney test. * $p < 0.05$, ** $p < 0.01$, *** $p < 0.001$.

After 7 days of cultivation, PDL 5% (median: 90.00% ± 32.50%) displayed significantly more epithelial cells than PDL 1% (median: 80.00% ± 65.00%, $p = 0.024$). Also, PDL 5% (median: 10.00% ± 35.00%) displayed significantly fewer ungrown areas than co 1% (median: 20.00% ± 80.00%, $p = 0.005$), co 5% (median: 20.00% ± 85.00%, $p = 0.045$), co 10% (median: 20.00% ± 65.00%, $p = 0.019$), or PDL 1% (median: 20.00% ± 75.00%, $p = 0.001$). PDL 10% (median: 15.00% ± 75.50%) had significantly fewer ungrown areas than PDL 1% ($p = 0.027$). After 14 days of cultivation, co 1% (median: 32.50% ± 72.25%) exhibited significantly fewer epithelial cells than co 5% (median: 80.00% ± 90.00%, $p = 0.038$) or PDL 5% (median: 90.00% ± 60.00%, $p < 0.001$). Co 1% (median: 40.00% ± 80.00%) displayed significantly more ungrown area than PDL 5% (median: 15.00% ± 62.50%, $p = 0.002$). After 28 days of cultivation, co 10% (median: 80.00% ± 78.75%) exhibited significantly more epithelial cells than PDL 10% (median: 30% ± 81.25%, $p < 0.001$). Overall, a 5% serum content is suitable for a good RPE morphology but does not generally outperform 10% serum.

3.3.4. Success Rates with Different Serum Content

Success rates for survival and confluence for all seeded wells for serum testing were determined. Of note, the general rate of survival was reduced to 53.70%, compared to 96,25% in the previous work package. The main difference in these packages was the season and quality of the eyes, as this work package was conducted in the late spring season of

2023 (refer to Section 2.1) in which the quality of the eyes and with it the success rate of the culture was reduced by unknown reasons, despite cooling the eyes during transportation. Usually, a reduction of RPE quality during the late spring or early summer season can be observed, which was especially noticeable in the year 2023. Success rates of all single-eye RPE cultures from serum testing were determined, depending on the coating (PDL or uncoated) and the serum content of the medium (1%, 5%, or 10%). The percentage of surviving cultures was calculated. Also, the percentage of wells from the surviving cultures that reached a confluence of 95–100% was determined (Table 7). PDL 5% had the highest success rate with a survival rate of 71.43% followed by co 5% with 59.42%. The lowest survival rate was achieved by co 1% with 42.03%. Concerning the confluence rate, PDL 10% had the highest success rate with 34.29% followed by PDL 5% with 31.43%. Again, co 1% showed the lowest success rate with 18.84%. Overall, PDL coating and 5% serum seem to be a good choice for successful single-eye RPE cultures but do not outperform PDL 10%.

Table 7. Success rates of cultures in different serum conditions. PDL = Poly-D-Lysine, co = uncoated control well, x% = serum content of medium, n = 417.

	co 1%	co 5%	co 10%	PDL 1%	PDL 5%	PDL 10%
survived	42.03	59.42	50.72	44.29	71.43	55.71
confluent	18.84	23.19	21.74	22.86	31.43	34.29

3.3.5. Growth Factor Secretion in Different Serum Conditions

To determine if the physiological growth factor secretion of VEGF-A is maintained with different serum content (1%, 5%, or 10%), supernatants of single-eye RPE culture were collected for 4 h on days 7, 14, and 28 after preparation and analyzed with ELISA (Figure 17). Cells were seeded on PDL or uncoated wells (co). After 28 days of cultivation, secreted VEGF ranged from 504.27 ± 171.99 pg/mL (co 1%) to 1104.05 ± 443.52 pg/mL (co 5%), which falls within the normal range of VEGF secretion of primary porcine mix culture RPE [39]. Co 5% secreted significantly more VEGF than co 1% (p = 0.015) or PDL 5% (mean: 582 ± 246 pg/mL, p = 0.029). After 7 days of cultivation, no significant differences were found. But, regarding 14 days, PDL 10% (mean: 754.21 ± 158.56 pg/mL) was significantly higher than co 10% (mean: 550.33 ± 65.29 pg/mL, p = 0.041) or PDL 1% (mean: 460.74 ± 189.28 pg/mL, p = 0.020). Also, PDL 5% (mean: 713.06 ± 233.49 pg/mL) was significantly higher than PDL 1% (mean: 460.74 ± 189.28 pg/mL, p = 0.027) and co 10% (mean: 550.33 ± 65.29 pg/mL, p = 0.045).

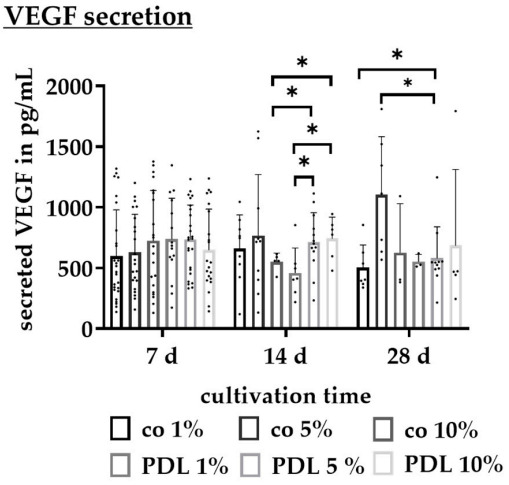

Figure 17. VEGF secretion in different serum conditions. Single-eye retinal pigment epithelium cells were seeded on Poly-D-Lysine (PDL) or uncoated wells (co) and cultivated in medium with 1%, 5%,

or 10% serum. Supernatants were collected for 24 h after 7, 14, and 28 days of cultivation and analyzed in ELISA for vascular endothelial growth factor A (VEGF-A). n = 3–26. Data were parametric; mean and standard deviation are shown. Significances were calculated between the groups with analysis of variance (ANOVA) and Student's t-test. * $p < 0.05$.

3.3.6. Protein Expression in Different Serum Conditions

Single-eye retinal pigment epithelium cells were seeded on PDL or uncoated wells (co) and treated with media containing 1%, 5%, or 10% serum. Protein expression of RPE65 and CLDN19 was investigated after 14 and 28 days of cultivation and analyzed with Western blotting (Figure 18 with example images).

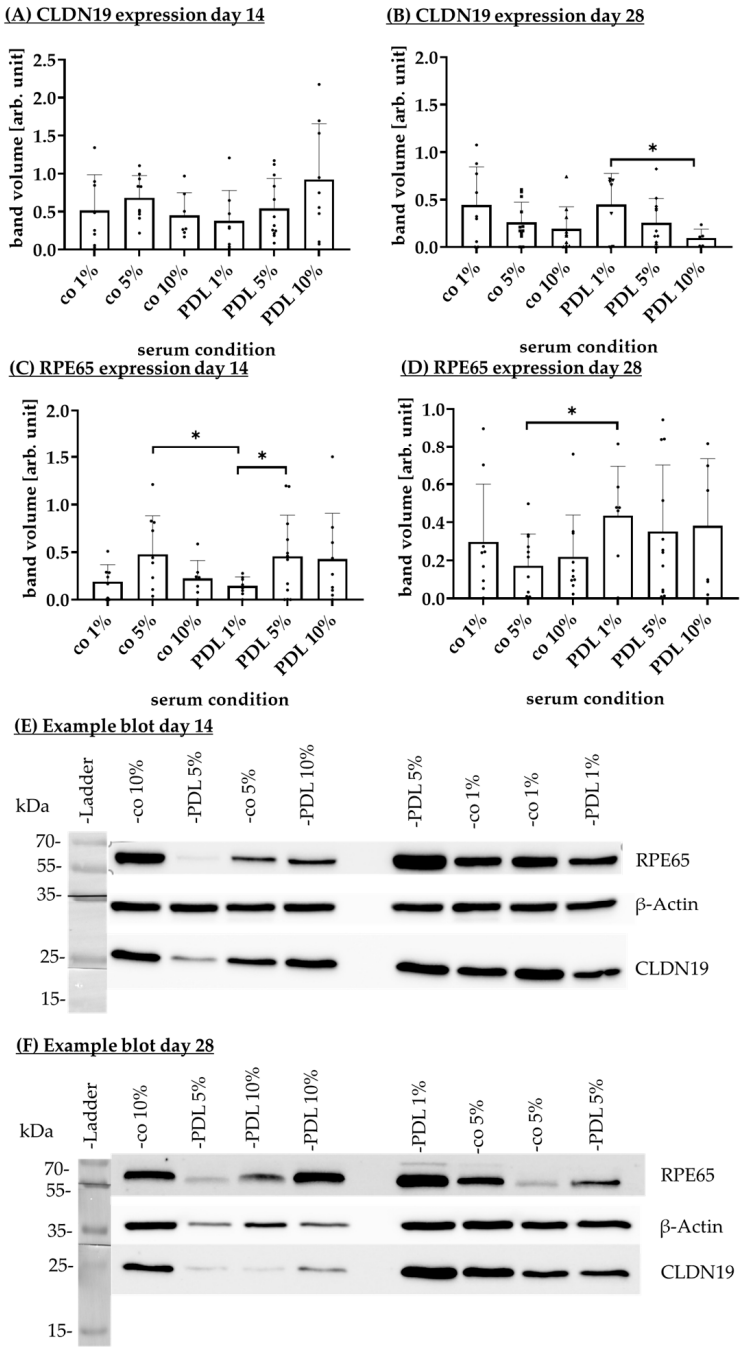

Figure 18. RPE65 and CLDN19 expression in different serum conditions. Single-eye retinal pigment epithelium cells were seeded on Poly-D-Lysine (PDL) or uncoated wells (co) and cultivated in medium

with 1%, 5%, or 10% serum. Lysates were made after 14 ((**A**), n = 7–12; (**C**), n = 7–12) and 28 days ((**B**), n = 5–12; (**D**), n = 6–12) of cultivation and analyzed with Western blotting for claudin-19 (CLDN19, (**A**,**B**)) and retinal pigment epithelium-specific 65 kDa protein (RPE65, (**C**,**D**)). Data were parametric; the mean of band volumes normalized to β-actin expression and standard deviation are depicted. Significances were calculated between each group with analysis of variance (ANOVA) and Student's t-test. * $p < 0.05$. (**E**,**F**) Exemplary blots for 14 and 28 days are depicted.

Regarding CLDN19 expression on day 14 (Figure 18A), no significant differences were observed. Descriptively, PDL 10% showed the highest CLDN19 expression (mean: 0.92 ± 0.73 [arb. unit]) and PDL 1% the lowest (mean: 0.38 ± 0.40 [arb. unit]). After 28 days of cultivation, CLDN19 expression (Figure 18B) was the highest with PDL 1% (mean: 0.45 ± 0.33 [arb. unit]), which was significantly higher than PDL 10% (mean: 0.10 ± 0.09 [arb. unit], $p = 0.044$). Independent of coating, CLDN19 expression decreased with increasing serum content.

RPE65 expression day 14 (Figure 18C) was highest in 5% serum and uncoated wells (mean: 0.48 ± 0.40 [arb. unit]), closely followed by 5% serum and PDL-coated wells (mean: 0.45 ± 0.43 [arb. unit]). PDL 1% showed the lowest RPE65 expression (mean: 0.14 ± 0.09 [arb. unit]), which was significantly lower than co 5% ($p = 0.030$) or PDL 5% ($p = 0.032$). After 28 days of cultivation (Figure 18D), PDL 1% displayed the highest expression (mean: 0.44 ± 0.26 [arb. unit]), which was significantly higher than co 5% (mean: 0.17 ± 0.17, $p = 0.015$).

Overall, the data indicate that after 14 days, these tight function and visual cycle proteins are more strongly expressed with higher serum content, while after long-term cultivation, lower serum content contributes to a higher protein expression.

3.3.7. Gene Expression

The gene expression pattern of single-eye RPE cultures was investigated with porcine-specific gene arrays for AMD and RPE-relevant genes [31] of our own design. The most suitable conditions determined in the former experiments were chosen (coating: PDL, serum content: 5%) and compared to the standard routine parameters (uncoated well (co), serum content 10%). RPE cells were seeded with conditions co 10%, co 5%, PDL 10%, or PDL 5% and cultivated for 28 days. All data and significances were calculated against standard condition co 10% (Rq = 1.000) and are listed in Appendix A Table A2. For a better overview, volcano plots are shown (Figure 19). Three flat gene expression changes were detected (significant values, but less than a 2-fold change). With PDL 10%, gene *CRYAB* was slightly up-regulated (Rq = 1.815, $p = 0.040$) and gene *VWF* was slightly down-regulated (Rq = 0.587, $p = 0.010$). With PDL 5%, gene *ANGPTL2* was slightly up-regulated (Rq = 1.657, $p = 0.039$). Clearly up-regulated (2-fold changed or higher) was proinflammatory and proangiogenic factor *CXCL8* with co 5% (Rq = 2.960, $p = 0.032$) and PDL 5% (Rq = 4.084, $p = 0.016$) conditions. Significances between other groups were not detected. Also, genes with more than a 2-fold expression change that did not reach significance are also highlighted in the volcano plots. Additionally, some genes were not expressed under specific conditions. Co 5% did not express *CRP* and *PLA2G2D*, and co 10% as a standard did not express *CRP*, *CX3CR1 PLA2G2D,* and *LEP*. PDL 5% and PDL 10% showed no expression of *CRP*, *CX3CR1*, or *PLA2G2D*, with the former also lacking an expression of *NOS1* and the latter lacking *FASLG*. Overall, the gene expression for all conditions is similar, only an up-regulation of *CXCL8* with 5% serum can be found. However, a general inflammatory response is not seen, as other inflammation-relevant genes were not influenced.

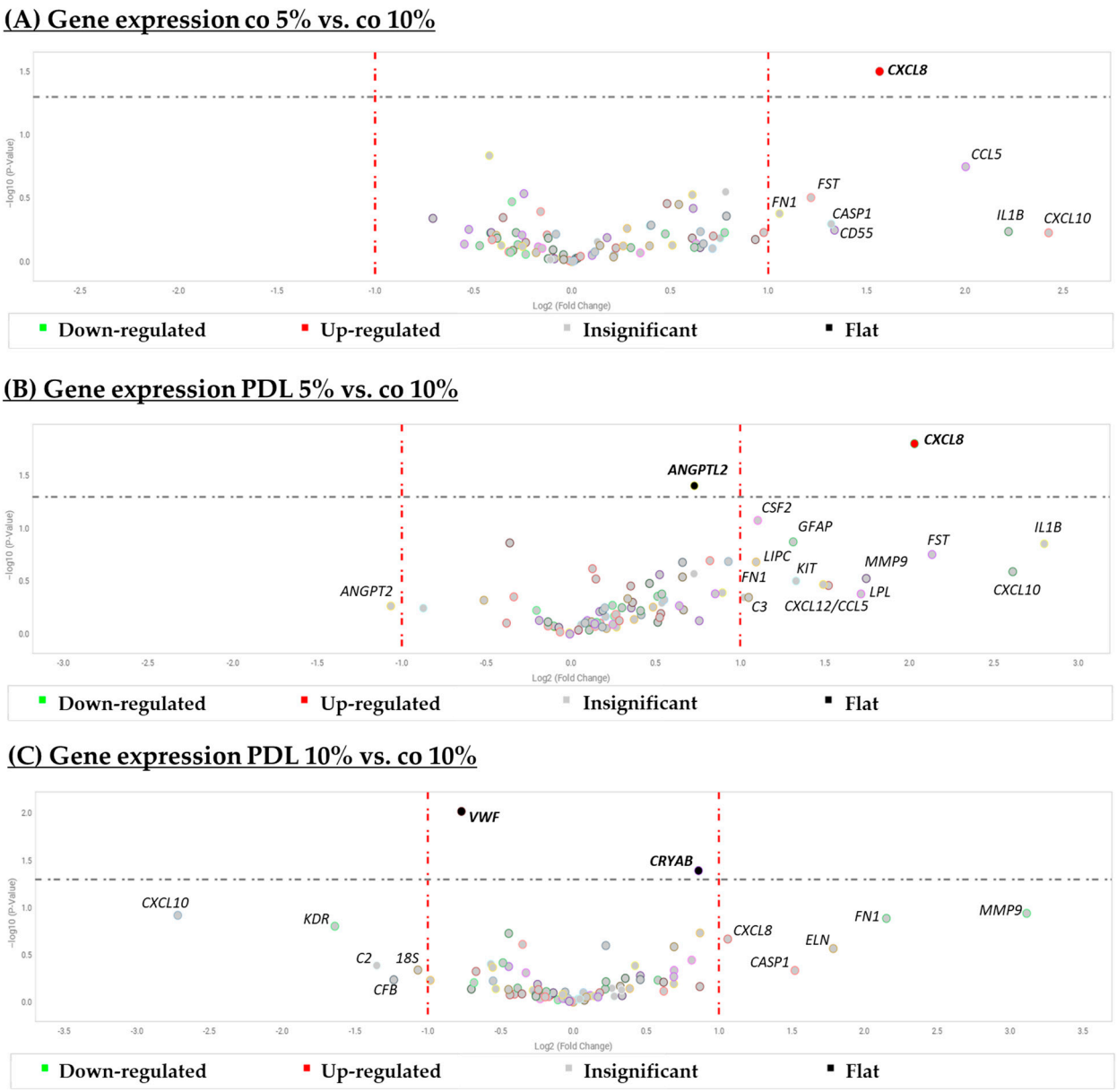

Figure 19. Gene expression in different serum conditions (volcano plots). Single-eye retinal pigment epithelium (RPE) cells were seeded on Poly-D-Lysine (PDL) or uncoated wells (co) and cultivated in a medium with 5% or 10% serum. RNA was isolated after 28 days of cultivation and analyzed with qPCR for different RPE-relevant genes. Relative quantification quotient (Rq) and significances were calculated between each group with analysis of variance (ANOVA) and Student's *t*-test by the cloud software Thermo Fisher Connect and are logarithmically shown. ((**A**), $n = 3$) Co 5% vs. co 10%, ((**B**), $n = 3$) PDL 5% vs. co 10%, ((**C**), $n = 3$) PDL 10% vs. co 10%. Gray dots = no significant gene regulation, black dots = significant flat gene expression regulation, red dots = significant up-regulation.

4. Discussion

One of the greatest obstacles in biomedical science is the lack of translational success "from bench to bedside" [41]. A major factor in this is the choice of models that are used in biomedical research. Often, the choice is made focusing on easy reproducibility and fast significance, with less focus on biological or medical relevance. In particular, the use of immortal cell lines with their convenient handling and their fast results [42] and the use of mouse models, which do not reflect the human situation and are often chosen

because of their availability [43], are part of the problem. This is even more prominent in ophthalmological research [7].

The use of porcine cell (and organ) culture is not new, and studies of porcine RPE cells are frequently published. However, there is still a lack of acceptance from the scientific community, especially considering reviewers of grant agencies and publications, but also by many researchers. The traditional use of mice is still very prominent [44], and lab material for mice (such as antibodies or primers) is highly available, while the availability of material for porcine tissue is limited. Porcine material is usually derived from animals killed for food production. These animals have a more heterogeneous background, considering both husbandry and genetic backgrounds, which will eventually lead to a higher variation of the experimental data [45]. Furthermore, cell culture techniques for porcine RPE are often traded down protocols, with various protocols in different labs that usually have not been validated for their efficiency (with some notable exceptions, e.g., [46]). In all published protocols, RPE cells of different eyes are mixed (e.g., [46–50]), so that cultures contain cells of different genetic origins, implying different responses in a given cell culture. Our RPE cell culture model uses a different approach. We use one eye for one culture, ensuring (1) genetic homogeneity in one culture and (2) genetic heterogeneity between cultures. This approach may lead to the need for a greater sample size to obtain significant results, but this approach ensures a higher biological relevance of the data. Indeed, it reflects the patient situation much more closely, as a patient is a genetically homogeneous entity while different patients will display different genotypes. Importantly, these cells are not passaged, avoiding the dedifferentiation that goes along with it [50–52]. Furthermore, we strictly evaluated the culture conditions to present a protocol based on scientific data, not a handed-down protocol. The major conditions we evaluated were PMT, coating, and serum content. The presented protocol is optimized for RPE cells grown on standard twelve-well cell culture dishes for studies not focusing on barrier functions. A protocol for RPE cells grown on transwell membranes optimized for barrier function is currently in preparation.

In our study, we could clearly show that 2 h PMT was not recommendable. Generally, a short PMT is considered beneficial for the culture, as the shorter the time, the less degeneration of the tissue has occurred; therefore, the better the quality. While this may still be true for organ cultures obtained from eyes, our results clearly show that a PMT of 2 h results in fewer successful cultures. The most likely explanation is that the RPE cells are more difficult to remove from their substrate at this early time point and that the early degenerative changes in the eye help the harvest of the cells. As the differences between 4 h and 6 h were rather small, we decided on a time window of 4 to 5 h PMT for all further experiments.

The results for the coating were rather surprising, as collagen turned out to be vastly inferior to other coatings. Collagen has been used frequently for RPE cell culture, including our own lab [53]. PDL showed to be the most appropriate coating, while no coating at all also showed very good results. PDL has been previously shown to enhance the growth of primary (bovine) RPE [54] and to enhance the attachment of (human) RPE cells compared to uncoated plates [55]. However, only a few studies concerning PDL have been published. The previous results from our group [56] indicated laminin as the most suitable coating for primary porcine RPE cells, but that study did not include PDL. As mentioned, a very interesting finding of our study is the inferiority of collagen compared to other coatings (or no coating at all). Collagen I has previously been shown to have no effect on RPE growth [54]. Another study that compared the outgrowth of human RPE did not find much difference between collagen I, collagen IV, or fibronectin, while laminin was associated with reduced growth [57]. Similarly, a recent study with primary porcine RPE did not see any effect of collagen I compared to uncoated regarding attachment, cell number, or

differentiation [46]. In accordance with our findings, however, Viheriälä et al. showed that the attachment of hESC-RPE on collagen IV was poor but was enhanced if laminin was added [58].

There are several aspects that may contribute to the different suitability of the different coating, such as mechanical, the stiffness of the coating [59], or biological properties, such as their ability to facilitate adhesion of the RPE cells [58]. Substrate stiffness has been shown to influence the properties of RPE cells [60], implicated, e.g., in fibrosis formation [61] or VEGF secretion [62]. However, other studies, including our own [56,63], found little influence of stiffness variation on RPE culture. On the other hand, the ability of cells to adhere to the extracellular matrix is of pronounced importance. While PDL is so far not commonly used for RPE culture, several studies showed an enhanced adhesion of neuronal cells to PDL coatings [64–66]. In addition, a recent paper on iPSC-derived RPE cells described a reduced adhesion of the RPE cells on collagen compared to a better adhesion on laminin (PDL was not tested), similar to our findings [58]. A better adhesion of the RPE is, therefore, likely to strongly contribute to the better performance of PDL and laminin.

To our knowledge, none of the published studies has compared the effect of these coatings on confluency, success, and morphology as we did, so to the best of our knowledge, this study is the first to provide scientific evidence for the suitability of different collagens, fibronectin, PDL, and laminin for primary porcine RPE cells. Our data suggest the use of PDL for coating. Most importantly, the use of collagen is discouraged by the data of our study. Of note, PDL is the only coating substance that has an artificial origin and comes not from animal resources, like laminin, collagens, or fibronectin, which is also an advantage regarding animal welfare.

We also determined the effect of serum content on cell number, confluency, success, morphology, and protein expression. Generally speaking, considering cell number, confluency, and success, 1% serum was inferior to 5% or 10%. This is in accordance with previously published data. For RPE cell culture, 10% serum is not uncommon (e.g., for rat RPE [67] or for human RPE [68]) and is used as a reference concentration if serum-free options are investigated (e.g., [69]). Indeed, a recent paper suggested 10% serum as the optimal concentration for porcine RPE cell culture [46]. Even studies that switch to 1% serum in (porcine) RPE cell culture have the cells proliferate for 7 days in 10% serum [48]. In accordance with our data, a paper studying wound healing in RPE cells found no difference between 5% and 10% serum but a reduction of wound healing in less serum [70]. Of interest, however, our data show a reduction of CLDN19 expression with increasing serum content, which is in accordance with studies that highly recommend serum reduction for a good tight junction formation in the RPE [48]. On the other hand, RPE65 expression (after 14 days) is inferior in 1% serum compared to 5% or 10%. Our data indicate that the nutrient requirement of the RPE cells differ between the proliferation and maturation of the cells and is in accordance with published data on RPE cell culture, which show that RPE cells proliferate in high serum but need lower serum content in culture in order to form tight junctions [67,71]. Our data indicate that both 10% and 5% are suitable for RPE cultivation, with 5% reducing the burden (both in costs and animal suffering) of FBS use.

Finally, we presented standard values for the morphometry of primary porcine RPE cells (area, perimeter, eccentricity, form factor, radius), which, to our knowledge, has not yet been presented before, providing a reference for all users of primary porcine RPE cells. A study conducted by Bhatia and colleagues examined the morphology of human RPE cells (from human donor eyes), and compared with these data, porcine RPE cells were similar in area and eccentricity to the human RPE of the far periphery ([72]; see also [19]). It would be of high interest to conduct a morphometry analysis in the pig's eye in situ to investigate

whether the different subpopulations of RPE cells that have recently been described in the human [19,73] can also be identified in the pig.

Taken together, we provide a validated protocol (Appendix B) for the use of single-eye RPE cells, including a reference for RPE cell morphology as an offer to the scientific community for a better model to investigate RPE cells. Further research will investigate amendments to these models for specific objectives.

5. Conclusions

The aim of this study was to create basic parameters for a standardized method protocol to generate and handle porcine single-eye retinal pigment epithelium cell culture, cultivating cells from one pig eye in one well of a twelve-well plate. This guarantees genetically homogenous cells in one culture and genetically heterogenous cells between cultures, enabling a higher relevance of the experimental data. This could be used for basic research for ophthalmologic diseases, such as age-related macular degeneration. Using pig eyes, which can be obtained as waste material, this study also contributes to the 3R principle. In addition, the porcine eye is genetically and anatomically closer to the human eye than the mouse eye. Within this study, we established parameters for post-mortem time, coating, and serum quantity of the culture medium. A post-mortem time of 4 to 5 h is optimal both in outcome and practicability. Coating with Poly-D-Lysine is recommended as it contributes to a better success rate, physiological differentiation, and cell parameters. For immunofluorescence purposes, however, coating coverslips should be avoided. Also, serum can be reduced to 5% as this may benefit the confluency, protein expression, and morphology of the RPE cells with the exception of a higher interleukin 8 gene expression. Taken together, basic parameters and a detailed protocol for the preparation and cultivation of porcine single-eye retinal pigment epithelium cultures have been established.

Author Contributions: Conceptualization, A.K.; methodology, A.K. and P.D.; software, J.W., N.T. and P.D.; validation, A.K., J.W., N.T. and P.D.; formal analysis, A.K., J.W., N.T. and P.D.; investigation, J.W., N.T. and P.D.; resources, A.K. and J.R.; data curation, A.K., J.W., N.T. and P.D.; writing—original draft preparation, A.K. and P.D.; writing—review and editing, A.K., J.R., J.W., N.T. and P.D.; visualization, A.K., J.W., N.T. and P.D.; supervision, A.K., J.R. and P.D.; project administration, A.K.; funding acquisition, A.K. All authors have read and agreed to the published version of the manuscript.

Funding: This research was funded by Bundesministerium für Bildung und Forschung, grant number 16LW0148.

Institutional Review Board Statement: The use of these eyes for experimental purposes was conducted in agreement with the animal welfare officer of the University of Kiel. According to the German Animal Welfare Act (TierSchG, https://www.gesetze-im-internet.de/tierschg (accessed on 8 February 2025)), this is not considered to be animal research but an alternative to the use of animals in research.

Informed Consent Statement: Not applicable.

Data Availability Statement: Data can be provided upon request.

Acknowledgments: Not applicable.

Conflicts of Interest: The authors declare no conflicts of interest. The funders had no role in the design of the study; in the collection, analyses, or interpretation of data; in the writing of the manuscript; or in the decision to publish the results.

Appendix A

Table A1. Influence of the quality of pigs' eyes on morphology. Single-eye retinal pigment epithelium cells were seeded for 7, 14, and 28 days. A portion of epithelial, mesenchymal, undivided cells, and ungrown areas of clear or bleared eyes was determined with light microscopy. n = 50–129. Data were not parametric; median and interquartile ranges were calculated.

Clear Eyes	Epithelial	Mesenchymal	Undivided	Ungrown
Day 7	61.67% ± 40.00%	6.67% ± 15.00%	3.33% ± 10.00%	10.00% ± 36.67%
Day 14	71.67% ± 30.00%	13.33% ± 25.00%	3.33% ± 10.00%	0.00% ± 3.33%
Day 28	70.00% ± 26.67%	16.67% ± 29.58%	3.33% ± 10.00%	0.00% ± 1.25%
Bleared Eyes				
Day 7	63.33% ± 34.17%	6.67% ± 8.33%	3.33% ± 10.00%	18.33% ± 36.67%
Day 14	73.33% ± 23.33%	11.67% ± 20.00%	3.33% ± 10.00%	0.00% ± 6.67%
Day 28	77.50% ± 31.25%	10.00% ± 30.00%	3.33% ± 10.00%	0.00% ± 0.42%

Table A2. Gene expression with different serum conditions, detailed data. Single-eye retinal pigment epithelium (RPE) cells were seeded on Poly-D-Lysine (PDL) or uncoated wells (co) and cultivated in a medium with 5% or 10% serum. RNA was isolated after 28 days of cultivation and analyzed via qPCR for different RPE-relevant genes. n = 3. Relative quantification quotient (Rq) with minimum (Rq Min) and maximum values (Rq Max) were calculated with Thermo Fisher Connect software. Significances were calculated between each group with analysis of variance (ANOVA) and Student's t-test of the cloud software Thermo Fisher Connect. * $p < 0.05$; no number available (used for normalization or no gene expression). Bold values are significant.

Bio Group Name	Target Name	Rq	Rq Min	Rq Max	p-Value (vs. co 10%)
co 10%	*18S*	1.000	0.911	1.098	1.000
co 10%	*ABCA4*	1.000	0.316	3.160	1.000
co 10%	*ACTG1*	-	-	-	-
co 10%	*ADRB2*	1.000	0.606	1.650	1.000
co 10%	*ANGPT2*	1.000	0.174	5.740	1.000
co 10%	*ANGPTL2*	1.000	0.935	1.070	1.000
co 10%	*ANXA5*	1.000	0.703	1.422	1.000
co 10%	*APOE*	1.000	0.501	1.994	1.000
co 10%	*BDNF*	1.000	0.677	1.477	1.000
co 10%	*BEST1*	1.000	0.261	3.831	1.000
co 10%	*C2*	1.000	0.210	4.769	1.000
co 10%	*C3*	1.000	0.335	2.984	1.000
co 10%	*C5*	1.000	0.501	1.996	1.000
co 10%	*C9*	1.000	0.339	2.953	1.000
co 10%	*CASP1*	1.000	0.266	3.756	1.000
co 10%	*CAT*	1.000	0.658	1.519	1.000
co 10%	*CCL2*	1.000	0.592	1.690	1.000
co 10%	*CCL5*	1.000	0.531	1.884	1.000
co 10%	*CD46*	1.000	0.817	1.224	1.000
co 10%	*CD55*	1.000	0.284	3.517	1.000
co 10%	*CD59*	1.000	0.578	1.731	1.000
co 10%	*CFB*	1.000	0.119	8.437	1.000
co 10%	*CFH*	1.000	0.408	2.450	1.000
co 10%	*CFI*	1.000	0.553	1.809	1.000
co 10%	*COL14A1*	1.000	0.566	1.767	1.000
co 10%	*CRP*	1.000	1.000	1.000	-
co 10%	*CRYAA*	1.000	0.480	2.082	1.000
co 10%	*CRYAB*	1.000	0.778	1.285	1.000
co 10%	*CSF2*	1.000	0.845	1.183	1.000
co 10%	*CST3*	1.000	0.711	1.407	1.000

Table A2. *Cont.*

Bio Group Name	Target Name	Rq	Rq Min	Rq Max	*p*-Value (vs. co 10%)
co 10%	*CTSD*	1.000	0.556	1.799	1.000
co 10%	*CX3CR1*	1.000	1.000	1.000	-
co 10%	*CXCL10*	1.000	0.286	3.492	1.000
co 10%	*CXCL12*	1.000	0.539	1.857	1.000
co 10%	*CXCL8*	1.000	0.645	1.551	1.000
co 10%	*DICER1*	1.000	0.811	1.233	1.000
co 10%	*ELN*	1.000	0.317	3.155	1.000
co 10%	*FASLG*	1.000	0.847	1.180	1.000
co 10%	*FLT1*	1.000	0.905	1.105	1.000
co 10%	*FMO1*	1.000	0.802	1.247	1.000
co 10%	*FN1*	1.000	0.333	3.007	1.000
co 10%	*FST*	1.000	0.589	1.697	1.000
co 10%	*GAPDH*	-	-	-	-
co 10%	*GFAP*	1.000	0.507	1.972	1.000
co 10%	*GPX4*	1.000	0.649	1.541	1.000
co 10%	*GSS*	1.000	0.947	1.056	1.000
co 10%	*GUSB*	-	-	-	-
co 10%	*HIF1A*	1.000	0.686	1.458	1.000
co 10%	*HMOX1*	1.000	0.581	1.722	1.000
co 10%	*HTRA1*	1.000	0.645	1.551	1.000
co 10%	*ICAM1*	1.000	0.711	1.406	1.000
co 10%	*IGF1*	1.000	0.228	4.385	1.000
co 10%	*IL1B*	1.000	0.475	2.107	1.000
co 10%	*IL1R2*	1.000	0.440	2.275	1.000
co 10%	*IL6*	1.000	0.604	1.655	1.000
co 10%	*IL6R*	1.000	0.667	1.500	1.000
co 10%	*KDR*	1.000	0.557	1.797	1.000
co 10%	*KIT*	1.000	0.561	1.782	1.000
co 10%	*LEP*	1.000	1.000	1.000	-
co 10%	*LIPC*	1.000	0.486	2.057	1.000
co 10%	*LPL*	1.000	0.157	6.353	1.000
co 10%	*MAPK1*	1.000	0.755	1.325	1.000
co 10%	*MAPK14*	1.000	0.951	1.052	1.000
co 10%	*MMP2*	1.000	0.586	1.707	1.000
co 10%	*MMP9*	1.000	0.222	4.502	1.000
co 10%	*MTOR*	1.000	0.654	1.53	1.000
co 10%	*NFE2L2*	1.000	0.798	1.253	1.000
co 10%	*NKAP*	1.000	0.888	1.126	1.000
co 10%	*NOS1*	1.000	0.836	1.197	1.000
co 10%	*NOS2*	1.000	0.561	1.784	1.000
co 10%	*PLA2G2D*	1.000	1.000	1.000	-
co 10%	*PTGS1*	1.000	0.710	1.408	1.000
co 10%	*PTGS2*	1.000	0.513	1.951	1.000
co 10%	*RDH11*	1.000	0.625	1.599	1.000
co 10%	*RLBP1*	1.000	0.391	2.556	1.000
co 10%	*RPE65*	1.000	0.352	2.839	1.000
co 10%	*SCARB1*	1.000	0.577	1.732	1.000
co 10%	*SERPINF1*	1.000	0.450	2.225	1.000
co 10%	*SERPING1*	1.000	0.706	1.416	1.000
co 10%	*SOD1*	1.000	0.750	1.333	1.000
co 10%	*SOD2*	1.000	0.656	1.525	1.000
co 10%	*SPARC*	1.000	0.576	1.736	1.000
co 10%	*TF*	1.000	0.400	2.503	1.000
co 10%	*TGFB1*	1.000	0.670	1.492	1.000
co 10%	*TIMP1*	1.000	0.889	1.125	1.000
co 10%	*TIMP3*	1.000	0.728	1.373	1.000
co 10%	*TLR2*	1.000	0.644	1.552	1.000
co 10%	*TLR3*	1.000	0.603	1.659	1.000
co 10%	*TLR4*	1.000	0.357	2.800	1.000

Table A2. *Cont.*

Bio Group Name	Target Name	Rq	Rq Min	Rq Max	*p*-Value (vs. co 10%)
co 10%	*TNF*	1.000	0.626	1.597	1.000
co 10%	*TYR*	1.000	0.469	2.134	1.000
co 10%	*VCAM1*	1.000	0.464	2.154	1.000
co 10%	*VEGFA*	1.000	0.628	1.593	1.000
co 10%	*VIM*	1.000	0.761	1.314	1.000
co 10%	*VLDLR*	1.000	0.586	1.706	1.000
co 10%	*VWF*	1.000	0.884	1.131	1.000
co 5%	*18S*	0.917	0.718	1.171	0.614
co 5%	*ABCA4*	0.723	0.234	2.237	0.745
co 5%	*ACTG1*	-	-	-	-
co 5%	*ADRB2*	0.941	0.261	3.391	0.945
co 5%	*ANGPT2*	0.927	0.183	4.690	0.959
co 5%	*ANGPTL2*	1.721	0.905	3.276	0.281
co 5%	*ANXA5*	0.840	0.549	1.286	0.616
co 5%	*APOE*	1.169	0.669	2.042	0.776
co 5%	*BDNF*	1.317	0.764	2.272	0.520
co 5%	*BEST1*	1.274	0.264	6.143	0.850
co 5%	*C2*	0.806	0.406	1.599	0.842
co 5%	*C3*	1.715	0.544	5.406	0.587
co 5%	*C5*	1.005	0.785	1.286	0.991
co 5%	*C9*	1.316	0.566	3.063	0.747
co 5%	*CASP1*	2.497	1.719	3.626	0.503
co 5%	*CAT*	0.966	0.669	1.397	0.921
co 5%	*CCL2*	1.591	0.234	10.802	0.720
co 5%	*CCL5*	4.012	1.186	13.572	0.178
co 5%	*CD46*	0.845	0.763	0.937	0.290
co 5%	*CD55*	2.527	0.295	21.629	0.562
co 5%	*CD59*	0.901	0.724	1.121	0.782
co 5%	*CFB*	1.541	0.654	3.631	0.769
co 5%	*CFH*	0.934	0.450	1.938	0.923
co 5%	*CFI*	0.850	0.616	1.172	0.704
co 5%	*COL14A1*	0.850	0.194	3.721	0.872
co 5%	*CRP*	0.988	0.854	1.143	-
co 5%	*CRYAA*	1.688	0.330	8.629	0.650
co 5%	*CRYAB*	1.105	0.728	1.678	0.744
co 5%	*CSF2*	1.726	0.651	4.574	0.435
co 5%	*CST3*	0.785	0.545	1.129	0.448
co 5%	*CTSD*	1.323	0.995	1.759	0.513
co 5%	*CXCL10*	5.374	0.059	488.817	0.590
co 5%	*CXCL12*	0.755	0.324	1.760	0.669
co 5%	***CXCL8***	**2.960**	**2.059**	**4.255**	**0.032 ***
co 5%	*DICER1*	1.095	0.808	1.484	0.695
co 5%	*ELN*	1.647	0.511	5.306	0.626
co 5%	*FASLG*	0.921	0.796	1.065	0.651
co 5%	*FLT1*	1.133	0.761	1.687	0.644
co 5%	*FMO1*	0.748	0.677	0.828	0.145
co 5%	*FN1*	2.080	0.891	4.856	0.416
co 5%	*FST*	2.325	0.795	6.801	0.311
co 5%	*GAPDH*	-	-	-	-
co 5%	*GFAP*	1.572	0.158	15.617	0.770
co 5%	*GPX4*	1.072	0.672	1.710	0.859
co 5%	*GSS*	1.032	0.694	1.533	0.904
co 5%	*GUSB*	-	-	-	-
co 5%	*HIF1A*	1.216	0.860	1.718	0.545
co 5%	*HMOX1*	0.882	0.367	2.120	0.845
co 5%	*HTRA1*	1.010	0.826	1.236	0.973
co 5%	*ICAM1*	1.400	0.916	2.140	0.347
co 5%	*IGF1*	1.162	0.967	1.397	0.877
co 5%	*IL1B*	4.667	0.283	77.010	0.577

Table A2. *Cont.*

Bio Group Name	Target Name	Rq	Rq Min	Rq Max	*p*-Value (vs. co 10%)
co 5%	*IL1R2*	0.769	0.535	1.105	0.650
co 5%	*IL6*	1.575	0.502	4.946	0.577
co 5%	*IL6R*	0.822	0.546	1.237	0.588
co 5%	*KDR*	0.780	0.274	2.219	0.742
co 5%	*KIT*	1.529	0.405	5.769	0.650
co 5%	*LIPC*	1.075	0.729	1.583	0.889
co 5%	*LPL*	1.643	0.170	15.841	0.784
co 5%	*MAPK1*	1.001	0.754	1.327	0.998
co 5%	*MAPK14*	0.946	0.812	1.103	0.605
co 5%	*MMP2*	1.232	0.449	3.379	0.772
co 5%	*MMP9*	1.969	0.542	7.150	0.586
co 5%	*MTOR*	0.767	0.374	1.573	0.618
co 5%	*NFE2L2*	1.014	0.836	1.231	0.939
co 5%	*NKAP*	0.971	0.736	1.282	0.878
co 5%	*NOS1*	0.896	0.869	0.924	0.402
co 5%	*NOS2*	0.972	0.502	1.879	0.958
co 5%	*PLA2G2D*	0.840	0.190	3.712	-
co 5%	*PTGS1*	1.551	0.251	9.577	0.719
co 5%	*PTGS2*	1.911	0.213	17.154	0.666
co 5%	*RDH11*	0.889	0.588	1.345	0.761
co 5%	*RLBP1*	0.813	0.281	2.349	0.813
co 5%	*RPE65*	0.685	0.173	2.717	0.725
co 5%	*SCARB1*	0.696	0.314	1.541	0.555
co 5%	*SERPINF1*	0.841	0.572	1.235	0.758
co 5%	*SERPING1*	0.992	0.739	1.331	0.977
co 5%	*SOD1*	1.021	0.774	1.346	0.934
co 5%	*SOD2*	1.085	0.681	1.729	0.833
co 5%	*SPARC*	0.753	0.403	1.406	0.587
co 5%	*TF*	0.801	0.194	3.301	0.832
co 5%	*TGFB1*	1.426	0.291	6.981	0.740
co 5%	*TIMP1*	1.199	0.510	2.823	0.749
co 5%	*TIMP3*	0.936	0.696	1.257	0.803
co 5%	*TLR2*	1.391	0.579	3.343	0.602
co 5%	*TLR3*	1.535	0.882	2.672	0.379
co 5%	*TLR4*	1.159	0.171	7.836	0.914
co 5%	*TNF*	0.827	0.503	1.361	0.732
co 5%	*TYR*	0.613	0.308	1.219	0.454
co 5%	*VCAM1*	0.920	0.165	5.130	0.944
co 5%	*VEGFA*	1.530	1.031	2.269	0.296
co 5%	*VIM*	0.810	0.676	0.971	0.336
co 5%	*VLDLR*	1.459	1.135	1.876	0.352
co 5%	*VWF*	0.751	0.345	1.637	0.591
PDL 10%	*18S*	0.477	0.118	1.932	0.456
PDL 10%	*ABCA4*	0.929	0.242	3.562	0.946
PDL 10%	*ACTG1*	-	-	-	-
PDL 10%	*ADRB2*	1.258	0.474	3.340	0.741
PDL 10%	*ANGPT2*	0.506	0.223	1.145	0.586
PDL 10%	*ANGPTL2*	1.757	0.770	4.010	0.358
PDL 10%	*ANXA5*	0.798	0.550	1.159	0.489
PDL 10%	*APOE*	0.890	0.349	2.272	0.872
PDL 10%	*BDNF*	1.376	0.623	3.037	0.577
PDL 10%	*BEST1*	1.261	0.279	5.690	0.852
PDL 10%	*C2*	0.392	0.378	0.408	0.409
PDL 10%	*C3*	0.623	0.212	1.832	0.622
PDL 10%	*C5*	0.825	0.414	1.644	0.750
PDL 10%	*C9*	0.981	0.711	1.354	0.979
PDL 10%	*CASP1*	2.871	0.809	10.191	0.461
PDL 10%	*CAT*	0.879	0.490	1.578	0.773
PDL 10%	*CCL2*	1.250	0.628	2.488	0.679

Table A2. *Cont.*

Bio Group Name	Target Name	Rq	Rq Min	Rq Max	*p*-Value (vs. co 10%)
PDL 10%	*CCL5*	0.675	0.591	0.772	0.396
PDL 10%	*CD46*	0.961	0.860	1.073	0.782
PDL 10%	*CD55*	1.538	0.225	10.502	0.764
PDL 10%	*CD59*	0.846	0.417	1.715	0.763
PDL 10%	*CFB*	0.425	0.143	1.260	0.580
PDL 10%	*CFH*	0.629	0.452	0.875	0.472
PDL 10%	*CFI*	0.681	0.432	1.076	0.428
PDL 10%	*COL14A1*	1.308	0.466	3.671	0.718
PDL 10%	*CRP*	1.047	0.568	1.929	-
PDL 10%	*CRYAA*	0.615	0.081	4.655	0.726
PDL 10%	***CRYAB***	**1.815**	**1.432**	**2.300**	**0.040 ***
PDL 10%	*CSF2*	1.167	1.071	1.272	0.351
PDL 10%	*CST3*	0.909	0.558	1.481	0.796
PDL 10%	*CTSD*	0.988	0.521	1.871	0.981
PDL 10%	*CX3CR1*	0.859	0.859	0.859	-
PDL 10%	*CXCL10*	0.152	0.142	0.163	0.120
PDL 10%	*CXCL12*	0.874	0.245	3.114	0.880
PDL 10%	*CXCL8*	2.087	1.028	4.236	0.214
PDL 10%	*DICER1*	1.031	0.637	1.670	0.926
PDL 10%	*ELN*	3.449	1.017	11.699	0.270
PDL 10%	*FASLG*	0.785	0.649	0.950	0.244
PDL 10%	*FLT1*	1.616	0.646	4.042	0.460
PDL 10%	*FMO1*	1.022	0.735	1.421	0.929
PDL 10%	*FN1*	4.442	2.349	8.398	0.129
PDL 10%	*FST*	1.826	0.205	16.227	0.684
PDL 10%	*GAPDH*	-	-	-	-
PDL 10%	*GFAP*	0.836	0.251	2.781	0.836
PDL 10%	*GPX4*	1.084	0.630	1.866	0.851
PDL 10%	*GSS*	1.049	0.799	1.377	0.793
PDL 10%	*GUSB*	-	-	-	-
PDL 10%	*HIF1A*	1.342	0.894	2.014	0.411
PDL 10%	*HMOX1*	1.376	0.770	2.458	0.525
PDL 10%	*HTRA1*	1.168	1.029	1.326	0.608
PDL 10%	*ICAM1*	0.887	0.393	2.003	0.831
PDL 10%	*IGF1*	1.613	1.102	2.363	0.639
PDL 10%	*IL1B*	1.215	0.246	6.002	0.867
PDL 10%	*IL1R2*	1.106	0.706	1.733	0.863
PDL 10%	*IL6*	0.767	0.282	2.087	0.709
PDL 10%	*IL6R*	0.846	0.440	1.629	0.730
PDL 10%	*KDR*	0.321	0.129	0.801	0.157
PDL 10%	*KIT*	1.537	0.468	5.051	0.614
PDL 10%	*LIPC*	0.999	0.415	2.401	0.998
PDL 10%	*LPL*	0.854	0.126	5.800	0.923
PDL 10%	*MAPK1*	0.974	0.757	1.252	0.909
PDL 10%	*MAPK14*	0.995	0.819	1.209	0.969
PDL 10%	*MMP2*	1.828	1.611	2.074	0.185
PDL 10%	*MMP9*	8.661	3.759	19.952	0.115
PDL 10%	*MTOR*	1.064	0.610	1.855	0.886
PDL 10%	*NFE2L2*	0.950	0.695	1.298	0.830
PDL 10%	*NKAP*	0.843	0.487	1.460	0.648
PDL 10%	*NOS1*	1.803	1.803	1.803	-
PDL 10%	*NOS2*	1.202	0.689	2.096	0.712
PDL 10%	*PLA2G2D*	0.258	0.258	0.258	-
PDL 10%	*PTGS1*	0.837	0.170	4.126	0.866
PDL 10%	*PTGS2*	0.783	0.171	3.587	0.817
PDL 10%	*RDH11*	0.735	0.516	1.047	0.419
PDL 10%	*RLBP1*	0.734	0.238	2.268	0.734
PDL 10%	*RPE65*	0.691	0.186	2.564	0.723
PDL 10%	*SCARB1*	0.847	0.471	1.522	0.738

Table A2. *Cont.*

Bio Group Name	Target Name	Rq	Rq Min	Rq Max	*p*-Value (vs. co 10%)
PDL 10%	*SERPINF1*	0.883	0.380	2.051	0.862
PDL 10%	*SERPING1*	0.715	0.445	1.148	0.383
PDL 10%	*SOD1*	0.964	0.605	1.536	0.914
PDL 10%	*SOD2*	1.134	0.590	2.180	0.796
PDL 10%	*SPARC*	1.281	0.883	1.859	0.559
PDL 10%	*TF*	0.739	0.090	6.038	0.835
PDL 10%	*TGFB1*	1.054	0.272	4.080	0.954
PDL 10%	*TIMP1*	1.059	0.472	2.378	0.914
PDL 10%	*TIMP3*	0.902	0.468	1.737	0.822
PDL 10%	*TLR2*	1.613	0.544	4.779	0.537
PDL 10%	*TLR3*	0.951	0.541	1.671	0.913
PDL 10%	*TLR4*	0.756	0.137	4.164	0.823
PDL 10%	*TNF*	1.496	0.559	4.001	0.585
PDL 10%	*TYR*	0.682	0.287	1.617	0.595
PDL 10%	*VCAM1*	1.125	0.411	3.081	0.880
PDL 10%	*VEGFA*	1.164	0.689	1.968	0.727
PDL 10%	*VIM*	0.735	0.703	0.767	0.187
PDL 10%	*VLDLR*	1.615	1.261	2.068	0.259
PDL 10%	***VWF***	**0.587**	**0.506**	**0.681**	**0.010 ***
PDL 5%	*18S*	1.092	1.046	1.141	0.240
PDL 5%	*ABCA4*	1.445	1.144	1.826	0.638
PDL 5%	*ACTG1*	-	-	-	-
PDL 5%	*ADRB2*	0.910	0.529	1.567	0.836
PDL 5%	*ANGPT2*	0.478	0.425	0.538	0.541
PDL 5%	***ANGPTL2***	**1.657**	**1.352**	**2.031**	**0.039 ***
PDL 5%	*ANXA5*	0.868	0.690	1.092	0.595
PDL 5%	*APOE*	1.105	0.712	1.717	0.844
PDL 5%	*BDNF*	1.438	1.069	1.933	0.273
PDL 5%	*BEST1*	1.438	0.899	2.301	0.694
PDL 5%	*C2*	0.995	0.581	1.704	0.996
PDL 5%	*C3*	2.070	0.742	5.773	0.448
PDL 5%	*C5*	1.464	0.947	2.264	0.472
PDL 5%	*C9*	0.956	0.603	1.514	0.951
PDL 5%	*CASP1*	1.427	1.139	1.786	0.769
PDL 5%	*CAT*	1.031	0.830	1.279	0.918
PDL 5%	*CCL2*	1.202	0.832	1.737	0.648
PDL 5%	*CCL5*	2.872	0.657	12.557	0.346
PDL 5%	*CD46*	0.993	0.859	1.149	0.966
PDL 5%	*CD55*	0.768	0.308	1.916	0.784
PDL 5%	*CD59*	0.995	0.911	1.086	0.989
PDL 5%	*CFB*	1.691	0.386	7.405	0.745
PDL 5%	*CFH*	1.078	0.554	2.098	0.913
PDL 5%	*CFI*	1.205	0.980	1.481	0.649
PDL 5%	*COL14A1*	1.905	1.203	3.017	0.205
PDL 5%	*CRP*	1.404	1.404	1.404	-
PDL 5%	*CRYAA*	0.546	0.128	2.334	0.566
PDL 5%	*CRYAB*	1.379	0.907	2.094	0.331
PDL 5%	*CSF2*	2.150	1.373	3.365	0.084
PDL 5%	*CST3*	1.185	0.916	1.533	0.532
PDL 5%	*CTSD*	1.280	0.949	1.726	0.563
PDL 5%	*CX3CR1*	0.928	0.928	0.928	-
PDL 5%	*CXCL10*	6.109	0.886	42.115	0.256
PDL 5%	*CXCL12*	2.810	0.681	11.597	0.338
PDL 5%	***CXCL8***	**4.084**	**2.702**	**6.173**	**0.016 ***
PDL 5%	*DICER1*	1.069	0.830	1.376	0.744
PDL 5%	*ELN*	1.586	0.806	3.119	0.589
PDL 5%	*FASLG*	0.864	0.864	0.864	-
PDL 5%	*FLT1*	1.124	0.806	1.569	0.611
PDL 5%	*FMO1*	1.194	0.648	2.200	0.675

Table A2. *Cont.*

Bio Group Name	Target Name	Rq	Rq Min	Rq Max	*p*-Value (vs. co 10%)
PDL 5%	*FN1*	2.030	0.784	5.261	0.448
PDL 5%	*FST*	4.390	1.206	15.984	0.176
PDL 5%	*GAPDH*	-	-	-	-
PDL 5%	*GFAP*	2.484	1.914	3.222	0.134
PDL 5%	*GPX4*	1.152	0.822	1.616	0.679
PDL 5%	*GSS*	0.935	0.545	1.602	0.849
PDL 5%	*GUSB*	-	-	-	-
PDL 5%	*HIF1A*	1.102	0.678	1.793	0.798
PDL 5%	*HMOX1*	1.137	0.433	2.986	0.853
PDL 5%	*HTRA1*	1.261	1.102	1.444	0.461
PDL 5%	*ICAM1*	1.277	1.075	1.517	0.350
PDL 5%	*IGF1*	1.205	0.587	2.473	0.857
PDL 5%	*IL1B*	6.951	1.708	28.296	0.139
PDL 5%	*IL1R2*	1.400	1.222	1.603	0.554
PDL 5%	*IL6*	1.330	0.663	2.669	0.599
PDL 5%	*IL6R*	1.031	0.865	1.229	0.912
PDL 5%	*KDR*	1.127	0.762	1.667	0.785
PDL 5%	*KIT*	2.514	0.773	8.170	0.313
PDL 5%	*LIPC*	2.135	1.414	3.224	0.207
PDL 5%	*LPL*	3.281	0.941	11.434	0.415
PDL 5%	*MAPK1*	0.791	0.542	1.156	0.443
PDL 5%	*MAPK14*	1.107	0.975	1.257	0.300
PDL 5%	*MMP2*	1.426	0.890	2.286	0.438
PDL 5%	*MMP9*	3.351	2.140	5.248	0.297
PDL 5%	*MTOR*	1.232	0.844	1.797	0.561
PDL 5%	*NFE2L2*	1.059	0.824	1.361	0.782
PDL 5%	*NKAP*	1.042	0.813	1.334	0.814
PDL 5%	*NOS1*	0.778	0.776	0.780	0.136
PDL 5%	*NOS2*	1.655	1.372	1.995	0.268
PDL 5%	*PLA2G2D*	2.646	1.941	3.607	-
PDL 5%	*PTGS1*	0.878	0.519	1.485	0.741
PDL 5%	*PTGS2*	1.860	0.738	4.691	0.404
PDL 5%	*RDH11*	0.910	0.835	0.992	0.764
PDL 5%	*RLBP1*	1.333	1.023	1.737	0.654
PDL 5%	*RPE65*	1.187	0.874	1.612	0.807
PDL 5%	*SCARB1*	1.11	1.049	1.175	0.774
PDL 5%	*SERPINF1*	1.451	1.314	1.602	0.506
PDL 5%	*SERPING1*	1.149	1.102	1.197	0.562
PDL 5%	*SOD1*	1.139	0.875	1.483	0.594
PDL 5%	*SOD2*	1.579	1.169	2.133	0.209
PDL 5%	*SPARC*	1.579	1.488	1.675	0.287
PDL 5%	*TF*	1.295	0.614	2.734	0.725
PDL 5%	*TGFB1*	1.805	0.676	4.814	0.414
PDL 5%	*TIMP1*	1.451	0.770	2.732	0.416
PDL 5%	*TIMP3*	0.951	0.672	1.346	0.863
PDL 5%	*TLR2*	1.287	0.870	1.903	0.500
PDL 5%	*TLR3*	1.097	0.816	1.476	0.801
PDL 5%	*TLR4*	1.157	0.342	3.917	0.882
PDL 5%	*TNF*	0.700	0.698	0.702	0.477
PDL 5%	*TYR*	1.219	0.658	2.257	0.744
PDL 5%	*VCAM1*	1.558	0.671	3.616	0.537
PDL 5%	*VEGFA*	1.110	0.791	1.559	0.770
PDL 5%	*VIM*	1.088	0.760	1.558	0.763
PDL 5%	*VLDLR*	1.767	1.543	2.023	0.201
PDL 5%	*VWF*	0.932	0.557	1.559	0.837

Table A3. Descriptive statistics for parametric data from the whole manuscript, sorted by the Figures they appear, with mean, standard deviation (Std Dev), minimum (Min), and maximum (Max).

Figure 3A	Cell Number × 10^5/mL	Mean	Std Dev	Min	Max
	0 d clear	3.31	6.96	0.05	72.80
	0 d bleared	2.56	3.62	0.00	33.35
	7 d clear	7.91	3.18	2.95	15.8
	7 d bleared	7.96	3.33	2.3	12.5
	14 d clear	8.37	3.83	2.65	18.3
	14 d bleared	8.58	3.83	2.95	17.85
	28 d clear	8.7	3.78	3.6	16.65
	28 d bleared	9.54	3.02	4.1	14.65
Figure 5A	**Cell Number × 10^5/mL**	**Mean**	**Std Dev**	**Min**	**Max**
	0 d 2 h	6.81	3.10	2.95	11.50
	0 d 4 h	9.85	2.69	2.30	15.55
	0 d 6 h	7.19	3.17	3.65	15.80
	7 d 2 h	9.43	3.45	4.50	17.85
	7 d 4 h	7.46	3.76	2.65	18.30
	7 d 6 h	7.70	2.25	4.10	12.55
	14 d 2 h	6.51	2.78	3.30	12.35
	14 d 4 h	9.30	2.81	3.60	12.70
	14 d 6 h	10.45	4.20	4.05	17.20
	28 d 2 h	9.68	3.03	7.00	17.00
	28 d 4 h	8.97	3.29	3.00	17.00
	28 d 6 h	9.73	3.06	3.00	18.00
Figure 7B	**Number of Cell Nuclei**	**Mean**	**Std Dev**	**Min**	**Max**
	2 h	499.20	161.08	104.00	778.00
	4 h	333.02	168.42	33.00	678.00
	6 h	361.07	114.30	172.00	557.00
Figure 8A	**Cell Number × 10^4/mL**	**Mean**	**Std Dev**	**Min**	**Max**
	7 d CIm	53.70	32.28	11.00	118.00
	7 d CIf	45.53	44.73	−5.50	141.50
	7 d CIV	32.03	29.68	−16.00	90.50
	7 d co	63.69	28.19	9.00	91.50
	14 d CIm	75.50	31.10	7.50	101.50
	14 d CIf	68.45	31.44	22.00	132.50
	14 d CIV	71.30	37.29	7.00	126.00
	14 d co	106.13	37.36	57.50	162.00
	28 d CIm	81.75	37.35	11.50	136.50
	28 d CIf	71.25	14.89	52.50	96.00
	28 d CIV	74.50	37.43	37.00	146.50
	28 d co	92.06	39.40	28.00	156.00
Figure 8B	**Cell Number × 10^4/mL**	**Mean**	**Std Dev**	**Min**	**Max**
	7 d CIm	39.20	29.91	−4.50	93.50
	7 d PDL	45.28	29.59	3.00	93.00
	7 d Lam	36.73	17.91	4.50	63.50
	7 d Fn	35.33	20.37	5.00	64.50
	7 d co	27.14	19.78	−1.50	62.50
	14 d CIm	58.66	27.76	8.00	127.50
	14 d PDL	81.31	30.11	33.00	115.00
	14 d Lam	74.86	35.69	30.00	161.00
	14 d Fn	68.40	25.32	24.50	106.00
	14 d co	50.50	32.74	10.00	112.50
	28 d CIm	51.95	33.23	−9.00	105.00
	28 d PDL	73.09	41.35	20.00	126.50
	28 d Lam	67.06	36.26	20.50	124.50
	28 d Fn	80.31	38.33	25.50	145.00
	28 d co	68.28	31.67	17.00	96.00

Table A3. *Cont.*

Figure 9A	% Cell Area per Well	Mean	Std Dev	Min	Max
	CIm	58.66	24.99	10.00	97.00
	CIf	39.85	26.65	5.00	85.00
	CIV	48.09	20.34	5.00	90.00
	co	85.62	24.32	20.00	100.00
Figure 11	**Secreted VEGF in pg/mL**	**Mean**	**Std Dev**	**Min**	**Max**
	7 d CIm	815.55	374.43	192	1484
	7 d PDL	845.84	214.59	504	1250
	7 d Lam	860.12	378.10	126	1587
	7 d Fn	851.98	312.60	373	1333
	7 d co	755.37	367.92	221	1156
	14 d CIm	928.89	328.42	266	1419
	14 d PDL	851.09	256.94	481	1322
	14 d Lam	984.51	292.95	587	1545
	14 d Fn	1012.96	380.95	469	1465
	14 d co	828.96	332.94	321	1314
	28 d CIm	828.56	369.46	139	1302
	28 d PDL	735.33	164.03	377	948
	28 d Lam	1038.50	248.47	631	1390
	28 d Fn	738.00	161.08	493	908
	28 d co	1109.33	276.78	652	1489
Figure 12A	**Band Volume [arb. unit]**	**Mean**	**Std Dev**	**Min**	**Max**
	CIm	0.67	0.55	0.08	1.42
	PDL	0.08	0.05	0.02	0.16
	Lam	1.74	4.08	0.01	10.98
	Fn	0.79	0.52	0.02	1.44
	co	0.42	0.19	0.24	0.69
Figure 12B	**Band Volume [arb. unit]**	**Mean**	**Std Dev**	**Min**	**Max**
	CIm	0.13	0.06	0.05	0.19
	PDL	0.14	0.06	0.05	0.19
	Lam	0.10	0.04	0.06	0.16
	Fn	0.17	0.04	0.11	0.23
	co	0.20	0.13	0.08	0.45
Figure 12C	**Band Volume [arb. unit]**	**Mean**	**Std Dev**	**Min**	**Max**
	CIm	0.27	0.37	0.01	0.93
	PDL	0.37	0.28	0.11	0.83
	Lam	0.08	0.10	0.00	0.26
	Fn	0.06	0.10	0.00	0.27
	co	0.37	0.36	0.00	0.90
Figure 12D	**Band Volume [arb. unit]**	**Mean**	**Std Dev**	**Min**	**Max**
	CIm	0.30	0.33	0.06	0.78
	PDL	0.29	0.25	0.11	0.79
	Lam	0.22	0.29	0.01	0.80
	Fn	0.23	0.15	0.08	0.50
	co	0.27	0.32	0.05	0.71

Table A3. *Cont.*

Figure 14A	Cell Number × 10^4/mL	Mean	Std Dev	Min	Max
	7 d co 1%	0.73	17.35	−25.50	40.50
	7 d co 5%	45.69	18.17	24.25	75.50
	7 d co 10%	59.73	17.85	34.50	93.75
	7 d PDL 1%	9.82	29.48	−41.00	65.00
	7 d PDL 5%	13.92	21.79	−21.50	52.00
	7 d PDL 10%	15.63	44.25	−84.50	66.00
	14 d co 1%	−7.71	25.12	−50.00	39.00
	14 d co 5%	17.30	27.12	−27.50	70.50
	14 d co 10%	42.15	25.90	4.50	93.00
	14 d PDL 1%	0.80	35.41	−80.50	71.50
	14 d PDL 5%	24.50	34.39	−45.00	76.50
	14 d PDL 10%	28.47	33.50	−18.00	89.50
	28 d co 1%	16.45	28.03	−23.50	78.00
	28 d co 5%	14.13	23.42	−38.00	49.50
	28 d co 10%	11.46	40.18	−75.00	80.50
	28 d PDL 1%	1.83	22.12	−43.50	40.50
	28 d PDL 5%	13.09	13.52	−9.00	34.00
	28 d PDL 10%	0.87	21.25	−40.50	38.00
Figure 17	**Secreted VEGF in pg/mL**	**Mean**	**Std Dev**	**Min**	**Max**
	7 d co 1%	599.26	372.12	139.00	1318.94
	7 d co 5%	628.73	306.83	158.31	1202.07
	7 d co 10%	724.82	404.72	130.75	1378.25
	7 d PDL 1%	739.12	324.92	174.28	1346.36
	7 d PDL 5%	737.11	276.33	332.69	1232.79
	7 d PDL 10%	650.19	327.03	143.62	1239.08
	14 d co 1%	660.66	261.45	121.08	1046.44
	14 d co 5%	767.13	478.09	134.21	1625.92
	14 d co 10%	550.33	65.29	427.07	616.28
	14 d PDL 1%	460.74	189.28	219.93	853.94
	14 d PDL 5%	713.06	233.49	234.28	1115.19
	14 d PDL 10%	745.21	158.56	479.08	945.15
	28 d co 1%	504.27	171.99	339.00	855.92
	28 d co 5%	1104.05	443.52	568.50	1811.31
	28 d co 10%	626.69	329.72	383.62	1092.85
	28 d PDL 1%	553.87	48.06	512.85	621.31
	28 d PDL 5%	582.12	245.63	214.92	1247.42
	28 d PDL 10%	685.62	560.79	245.92	1794.38
Figure 18A	**Band Volume [arb. unit]**	**Mean**	**Std Dev**	**Min**	**Max**
	co 1%	0.51	0.47	0.03	1.34
	co 5%	0.68	0.29	0.22	1.11
	co 10%	0.45	0.30	0.17	0.97
	PDL 1%	0.38	0.40	0.01	1.21
	PDL 5%	0.54	0.39	0.09	1.17
	PDL 10%	0.92	0.73	0.07	2.17
Figure 18B	**Band Volume [arb. unit]**	**Mean**	**Std Dev**	**Min**	**Max**
	co 1%	0.44	0.40	0.00	1.08
	co 5%	0.26	0.21	0.00	0.60
	co 10%	0.19	0.23	0.00	0.74
	PDL 1%	0.45	0.33	0.00	0.72
	PDL 5%	0.25	0.26	0.00	0.82
	PDL 10%	0.10	0.09	0.01	0.24

Table A3. *Cont.*

Figure 18C	Band Volume [arb. unit]	Mean	Std Dev	Min	Max
	co 1%	0.19	0.18	0.00	0.51
	co 5%	0.48	0.40	0.00	1.21
	co 10%	0.22	0.19	0.00	0.59
	PDL 1%	0.14	0.09	0.00	0.28
	PDL 5%	0.45	0.43	0.00	1.20
	PDL 10%	0.43	0.48	0.00	1.50
Figure 18D	**Band Volume [arb. unit]**	**Mean**	**Std Dev**	**Min**	**Max**
	co 1%	0.30	0.30	0.00	0.90
	co 5%	0.17	0.17	0.00	0.50
	co 10%	0.22	0.22	0.02	0.76
	PDL 1%	0.44	0.26	0.00	0.82
	PDL 5%	0.35	0.35	0.01	0.94
	PDL 10%	0.38	0.35	0.02	0.82

Appendix B. Preparation of Porcine Single-Eye Retinal Pigment Epithelium (Full Protocol)

Appendix B.1. Materials

- Freshly slaughtered pig eyes (kept on ice)
- Water bath
- Safety workbench
- Cell incubator
- Centrifuge
- 1000 µL pipettes
- Twelve-well polystyrene plate for adherent cells (e.g., Sarstedt; #83.3921)
- Optional: sterile coverslips (Th. Geyer; #CB00180RA1)
- Styrofoam box
- Crushed ice
- 500 mL sterile glass beaker
- 250 mL and 500 mL sterile plastic beakers
- Pressure seal bags (small and big)
- Sterile 15 mL and 50 mL tubes
- Underlays
- Clothes
- Sterile preparation set with
    - Enucleation scissors
    - Microspring scissors
    - Long curved forceps
    - Small straight tweezers
    - Small straight tweezers with a hook
- Sterile razor blades
- Sterile medium-sized and big glass Petri dishes
- Lab bottle lids (fitting the size of one pig eye)
- 0.9% sterile NaCl (e.g., Fresenius Kabi; #04801702)
- Sterile iodine solution (e.g., Betaisodona®; #04923204) diluted 1:3 with 0.9% NaCl
- 70% ethanol
- Poly-D-Lysine (PDL, e.g., Sigma-Aldrich; #P7886)
- Sterile trypsin solution (T, 0.25 g T/100 mL PBS, e.g., Pan-Biotech; #P10-021100)

- Sterile trypsin/EDTA solution (T/E, 0.05 g T + 0.02 g EDTA/100 mL PBS, e.g., Pan-Biotech; #P10-020100)
- Sterile Dulbecco's phosphate-buffered saline without Ca and Mg (e.g., Pan-Biotech; #P04-53500) with 1% penicillin/streptomycin (e.g., Sigma-Aldrich; #P0781) → PBS + Pe/St
- Cell media containing
    - Dulbecco's Modified Eagle Medium with high glucose, L-glutamine, and phenol red (DMEM, Gibco™, Thermo Fisher Scientific; #41965062)
    - 1% non-essential amino acids (Pan-Biotech; #P08-32100)
    - 11 mM sodium pyruvate (Pan-Biotech; #P04-43100)
    - 1% penicillin/streptomycin (Sigma-Aldrich; #P0781)
    - 10% or 5% fetal bovine serum (FBS, Gibco™, Thermo Fisher Scientific; #10437028)

Appendix B.2. First Things to Prepare

Working place in the lab

1. Put crushed ice in the Styrofoam box and place a glass beaker filled with 250 mL of 0.9% NaCl
2. Put aliquoted iodine solution on ice (50 mL tube)
3. Put an underlay with an EtOH moisture cloth on it
4. Have an organic waste bag ready
5. Place the preparation set
6. Put in a 37 °C warm water bath
7. One aliquot of T (50 mL in 50 mL tube) for 12 eyes
8. One aliquot of T/E (50 mL in 50 mL tube) for 12 eyes
9. One aliquot of PBS + Pe/St (50 mL in 50 mL tube) for 12 eyes
10. Cell media
11. Bench
12. EtOH moisture cloth with a sterile razor blade
13. One big glass Petri dish filled with bottle lids
14. One smaller glass Petri dish
15. Waste bags in plastic beakers, one for organic waste and one for plastic waste
16. For immune staining, add sterile coverslips into the wells of the twelve-well plate and do not coat them
17. For other assays, coat the wells of the twelve-well plate with PDL as described by the manufacturer's instructions

Appendix B.3. In the Lab

Preparation process

1. Start 4 to 5 h after the first pig was slaughtered.
2. Remove muscles, fat, conjunctiva, and excess connective tissue from the eyes with enucleation scissors on top of the cloth. Roughly trim the optic nerve (do not cut too close).
3. Place three eyes at a time in the tube with iodine solution (on ice) for approx. 5 min.
4. Transfer the eyes into cold 0.9% NaCl in a glass beaker until all eyes are fully prepared.

Appendix B.4. Under the Bench

Preparation process

5. For the preparation process, use media with 10% FBS.

6. Put one eye in the smaller Petri dish and cut the eye approx. 3 mm below the ciliary body with the razor blade and cut around it once with the enucleation scissors to create an eye cup.
7. Remove the lens and the vitreous body by putting the enucleation scissors into the vitreous body, open the scissors and pull it out, so that the eye is a small open bowl.
8. Fill the eye cup with warm PBS + Pe/St and carefully loosen the retina with the tweezers and microscissors (carefully hold the eye from the outside with the tweezer with hook and pull the retina with the other tweezer from the top to the center and cut off at the optic nerve with the microscissors). Remove the retina.
9. Remove PBS + Pe/St and place the eye cups in the lids. Do not leave the Petri dish open for long (avoid drying out the eyes).
10. Add approx. 3 mL T (ready aliquoted) to the eye dishes and incubate at 37 °C for 10 min in the closed Petri dish.
11. Remove T and add approx. 3 mL T/E (ready aliquoted) to the eye cups.
12. Incubate at 37 °C for exactly 35 min in the closed Petri dish.
13. Dissolve the RPE cells from the choroid by pipetting up and down with the 1000 µL pipette (set to 800 µL, rinse the eye carefully exactly 30 times, dividing each time equally between the center and the edges).
14. After all eyes have been resuspended, transfer cells into prepared 15 mL tubes (filled with 1 mL medium) and fill up to 5 mL volume with medium to neutralize the T/E.
15. Centrifuge for 5 min at 200× *g*.
16. Carefully aspirate the supernatant (keep the tube slightly tilted, the pellet is sensitive).
17. Resuspend each pellet in 1 mL of fresh RPE medium. Fill up to a volume of 5 mL with fresh medium and centrifuge again for 5 min at 200× *g*.
18. Resuspend the pellet in 1000 µL medium.
19. Pipette the cell suspension in a circle into the respective well of the twelve-well plate. Swirl the plate once more (to ensure even distribution of the cells in the well) and place it in the incubator (humidified, 37 °C, 5% CO_2).
20. After 3 to 4 days, change to media with 5% FBS and renew every 3 to 4 days.

References

1. Wong, W.L.; Su, X.; Li, X.; Cheung, C.M.G.; Klein, R.; Cheng, C.-Y.; Wong, T.Y. Global prevalence of age-related macular degeneration and disease burden projection for 2020 and 2040: A systematic review and meta-analysis. *Lancet Glob. Health* **2014**, *2*, e106–e116. [CrossRef] [PubMed]
2. Zając-Pytrus, H.M.; Pilecka, A.; Turno-Kręcicka, A.; Adamiec-Mroczek, J.; Misiuk-Hojło, M. The Dry Form of Age-Related Macular Degeneration (AMD): The Current Concepts of Pathogenesis and Prospects for Treatment. *Adv. Clin. Exp. Med.* **2015**, *24*, 1099–1104. [CrossRef] [PubMed]
3. Fleckenstein, M.; Keenan, T.D.L.; Guymer, R.H.; Chakravarthy, U.; Schmitz-Valckenberg, S.; Klaver, C.C.; Wong, W.T.; Chew, E.Y. Age-related macular degeneration. *Nat. Rev. Dis. Primers* **2021**, *7*, 31. [CrossRef]
4. Bhutto, I.; Lutty, G. Understanding age-related macular degeneration (AMD): Relationships between the photoreceptor/retinal pigment epithelium/Bruch's membrane/choriocapillaris complex. *Mol. Asp. Med.* **2012**, *33*, 295–317. [CrossRef]
5. Strauss, O. The retinal pigment epithelium in visual function. *Physiol. Rev.* **2005**, *85*, 845–881. [CrossRef]
6. Aisenbrey, S.; Zhang, M.; Bacher, D.; Yee, J.; Brunken, W.J.; Hunter, D.D. Retinal pigment epithelial cells synthesize laminins, including laminin 5, and adhere to them through alpha3-and alpha6-containing integrins. *Investig. Ophthalmol. Vis. Sci.* **2006**, *47*, 5537–5544. [CrossRef]
7. Schnichels, S.; Paquet-Durand, F.; Löscher, M.; Tsai, T.; Hurst, J.; Joachim, S.C.; Klettner, A. Retina in a dish: Cell cultures, retinal explants and animal models for common diseases of the retina. *Prog. Retin. Eye Res.* **2021**, *81*, 100880. [CrossRef]
8. Bharti, K.; den Hollander, A.I.; Lakkaraju, A.; Sinha, D.; Williams, D.S.; Finnemann, S.C.; Bowes-Rickman, C.; Malek, G.; D'Amore, P.A. Cell culture models to study retinal pigment epithelium-related pathogenesis in age-related macular degeneration. *Exp. Eye Res.* **2022**, *222*, 109170. [CrossRef]

9. Alge, C.S.; Hauck, S.M.; Priglinger, S.G.; Kampik, A.; Ueffing, M. Differential protein profiling of primary versus immortalized human RPE cells identifies expression patterns associated with cytoskeletal remodeling and cell survival. *J. Proteome Res.* **2006**, *5*, 862–878. [CrossRef]
10. Dunn, K.C.; Aotaki-Keen, A.E.; Putkey, F.R.; Hjelmeland, L.M. ARPE-19, a human retinal pigment epithelial cell line with differentiated properties. *Exp. Eye Res.* **1996**, *62*, 155–169. [CrossRef]
11. Tian, J.; Ishibashi, K.; Honda, S.; Boylan, S.A.; Hjelmeland, L.M.; Handa, J.T. The expression of native and cultured human retinal pigment epithelial cells grown in different culture conditions. *Br. J. Ophthalmol.* **2005**, *89*, 1510–1517. [CrossRef] [PubMed]
12. Ahmado, A.; Carr, A.-J.; Vugler, A.A.; Gias, C.; Lawrence, J.M.; Chen, L.L.; Chen, F.K.; Turowski, P.; da Cruz, L.; Coffey, P.J. Induction of differentiation by pyruvate and DMEM in the human retinal pigment epithelium cell line ARPE-19. *Investig. Ophthalmol. Vis. Sci.* **2011**, *52*, 7148–7159. [CrossRef] [PubMed]
13. Samuel, W.; Jaworski, C.; Postnikova, O.A.; Kutty, R.K.; Duncan, T.; Tan, L.X.; Poliakov, E.; Lakkaraju, A.; Redmond, T.M. Appropriately differentiated ARPE-19 cells regain phenotype and gene expression profiles similar to those of native RPE cells. *Mol. Vis.* **2017**, *23*, 60–89. [PubMed]
14. Golconda, P.; Andrade-Medina, M.; Oberstein, A. Subconfluent ARPE-19 Cells Display Mesenchymal Cell-State Characteristics and Behave like Fibroblasts, Rather Than Epithelial Cells, in Experimental HCMV Infection Studies. *Viruses* **2023**, *16*, 49. [CrossRef]
15. Luo, Y.; Zhuo, Y.; Fukuhara, M.; Rizzolo, L.J. Effects of culture conditions on heterogeneity and the apical junctional complex of the ARPE-19 cell line. *Investig. Ophthalmol. Vis. Sci.* **2006**, *47*, 3644–3655. [CrossRef]
16. Nakai-Futatsugi, Y.; Jin, J.; Ogawa, T.; Sakai, N.; Maeda, A.; Hironaka, K.-I.; Fukuda, M.; Danno, H.; Tanaka, Y.; Hori, S.; et al. Pigmentation level of human iPSC-derived RPE does not indicate a specific gene expression profile. *eLife* **2024**, *12*, RP92510. [CrossRef]
17. Farjood, F.; Manos, J.D.; Wang, Y.; Williams, A.L.; Zhao, C.; Borden, S.; Alam, N.; Prusky, G.; Temple, S.; Stern, J.H.; et al. Identifying biomarkers of heterogeneity and transplantation efficacy in retinal pigment epithelial cells. *J. Exp. Med.* **2023**, *220*, e20230913. [CrossRef]
18. Miyagishima, K.J.; Wan, Q.; Corneo, B.; Sharma, R.; Lotfi, M.R.; Boles, N.C.; Hua, F.; Maminishkis, A.; Zhang, C.; Blenkinsop, T.; et al. In Pursuit of Authenticity: Induced Pluripotent Stem Cell-Derived Retinal Pigment Epithelium for Clinical Applications. *Stem Cells Transl. Med.* **2016**, *5*, 1562–1574. [CrossRef]
19. Rzhanova, L.A.; Markitantova, Y.V.; Aleksandrova, M.A. Recent Achievements in the Heterogeneity of Mammalian and Human Retinal Pigment Epithelium: In Search of a Stem Cell. *Cells* **2024**, *13*, 281. [CrossRef]
20. Luo, M.; Chen, Y. Application of stem cell-derived retinal pigmented epithelium in retinal degenerative diseases: Present and future. *Int. J. Ophthalmol.* **2018**, *11*, 150–159.
21. Nguyen, H.V.; Li, Y.; Tsang, S.H. Patient-Specific iPSC-Derived RPE for Modeling of Retinal Diseases. *J. Clin. Med.* **2015**, *4*, 567–578. [CrossRef] [PubMed]
22. Dalvi, S.; Galloway, C.A.; Singh, R. Pluripotent Stem Cells to Model Degenerative Retinal Diseases: The RPE Perspective. *Adv. Exp. Med. Biol.* **2019**, *1186*, 1–31. [PubMed]
23. Mandai, M.; Watanabe, A.; Kurimoto, Y.; Hirami, Y.; Morinaga, C.; Daimon, T.; Fujihara, M.; Akimaru, H.; Sakai, N.; Shibata, Y.; et al. Autologous Induced Stem-Cell-Derived Retinal Cells for Macular Degeneration. *New Engl. J. Med.* **2017**, *376*, 1038–1046. [CrossRef]
24. Ke, Q.; Gong, L.; Zhu, X.; Qi, R.; Zou, M.; Chen, B.; Liu, W.; Huang, S.; Liu, Y.; Li, D.W.-C. Multinucleated Retinal Pigment Epithelial Cells Adapt to Vision and Exhibit Increased DNA Damage Response. *Cells* **2022**, *11*, 1552. [CrossRef]
25. Rizzolo, L.J. Barrier properties of cultured retinal pigment epithelium. *Exp. Eye Res.* **2014**, *126*, 16–26. [CrossRef]
26. Sanchez, I.; Martin, R.; Ussa, F.; Fernandez-Bueno, I. The parameters of the porcine eyeball. *Graefe's Arch. Clin. Exp. Ophthalmol.* **2011**, *249*, 475–482. [CrossRef]
27. Middleton, S. Porcine ophthalmology. *Vet. Clin. North America. Food Anim. Pract.* **2010**, *26*, 557–572. [CrossRef]
28. Degroote, R.L.; Schmalen, A.; Renner, S.; Wolf, E.; Hauck, S.M.; Deeg, C.A. Diabetic retinopathy from the vitreous proteome perspective: The INSC94Y transgenic pig model study. *Proteomics* **2024**, *24*, e2300591. [CrossRef]
29. Ng, Y.-F.; Chan, H.H.L.; Chu, P.H.W.; To, C.-H.; Gilger, B.C.; Petters, R.M.; Wong, F. Multifocal electroretinogram in rhodopsin P347L transgenic pigs. *Investig. Ophthalmol. Vis. Sci.* **2008**, *49*, 2208–2215. [CrossRef]
30. Klettner, A.; Roider, J. Comparison of bevacizumab, ranibizumab, and pegaptanib in vitro: Efficiency and possible additional pathways. *Investig. Ophthalmol. Vis. Sci.* **2008**, *49*, 4523–4527. [CrossRef]
31. Dörschmann, P.; Akkurt, H.; Kopplin, G.; Mikkelsen, M.D.; Meyer, A.S.; Roider, J.; Klettner, A. Establishment of specific age-related macular degeneration relevant gene expression panels using porcine retinal pigment epithelium for assessing fucoidan bioactivity. *Exp. Eye Res.* **2023**, *231*, 109469. [CrossRef] [PubMed]
32. MacArthur Clark, J. The 3Rs in research: A contemporary approach to replacement, reduction and refinement. *Br. J. Nutr.* **2018**, *120*, S1–S7. [CrossRef] [PubMed]

33. Kiamehr, M.; Klettner, A.; Richert, E.; Koskela, A.; Koistinen, A.; Skottman, H.; Kaarniranta, K.; Aalto-Setälä, K.; Juuti-Uusitalo, K. Compromised Barrier Function in Human Induced Pluripotent Stem-Cell-Derived Retinal Pigment Epithelial Cells from Type 2 Diabetic Patients. *Int. J. Mol. Sci.* **2019**, *20*, 3773. [CrossRef]
34. Liu, D.; Zhang, C.; Zhang, J.; Xu, G.-T.; Zhang, J. Molecular pathogenesis of subretinal fibrosis in neovascular AMD focusing on epithelial-mesenchymal transformation of retinal pigment epithelium. *Neurobiol. Dis.* **2023**, *185*, 106250. [CrossRef]
35. Kaarniranta, K.; Blasiak, J.; Liton, P.; Boulton, M.; Klionsky, D.J.; Sinha, D. Autophagy in age-related macular degeneration. *Autophagy* **2023**, *19*, 388–400. [CrossRef]
36. Duncan, R.S.; Keightley, A.; Lopez, A.A.; Hall, C.W.; Koulen, P. Proteomics Analysis on the Effects of Oxidative Stress and Antioxidants on Proteins Involved in Sterol Transport and Metabolism in Human Telomerase Transcriptase-Overexpressing-Retinal Pigment Epithelium Cells. *Int. J. Mol. Sci.* **2024**, *25*, 10893. [CrossRef]
37. Livak, K.J.; Schmittgen, T.D. Analysis of relative gene expression data using real-time quantitative PCR and the 2(-Delta Delta C(T)) Method. *Methods* **2001**, *25*, 402–408. [CrossRef]
38. Dithmer, M.; Kirsch, A.-M.; Richert, E.; Fuchs, S.; Wang, F.; Schmidt, H.; Coupland, S.E.; Roider, J.; Klettner, A. Fucoidan Does Not Exert Anti-Tumorigenic Effects on Uveal Melanoma Cell Lines. *Mar. Drugs* **2017**, *15*, 193. [CrossRef]
39. Dörschmann, P.; Kopplin, G.; Roider, J.; Klettner, A. Effects of Sulfated Fucans from Laminaria hyperborea Regarding VEGF Secretion, Cell Viability, and Oxidative Stress and Correlation with Molecular Weight. *Mar. Drugs* **2019**, *17*, 548. [CrossRef]
40. Klettner, A.K.; Dithmar, S. *Retinal Pigment Epithelium in Health and Disease*; Springer: Cham, Switzerland, 2020.
41. Seyhan, A.A. Lost in translation: The valley of death across preclinical and clinical divide—identification of problems and overcoming obstacles. *Transl. Med. Commun.* **2019**, *4*, 18. [CrossRef]
42. Saeidnia, S.; Manayi, A.; Abdollahi, M. From in vitro Experiments to in vivo and Clinical Studies; Pros and Cons. *Curr. Drug Discov. Technol.* **2015**, *12*, 218–224. [CrossRef] [PubMed]
43. Leist, M.; Hartung, T. Inflammatory findings on species extrapolations: Humans are definitely no 70-kg mice. *Arch. Toxicol.* **2013**, *87*, 563–567. [CrossRef] [PubMed]
44. Veening-Griffioen, D.H.; Ferreira, G.S.; Boon, W.P.C.; Gispen-de Wied, C.C.; Schellekens, H.; Moors, E.H.M.; van Meer, P.J.K. Tradition, not science, is the basis of animal model selection in translational and applied research. *Altex* **2021**, *38*, 49–62. [CrossRef] [PubMed]
45. Berg, C.; Wilker, S.; Roider, J.; Klettner, A. Isolation of porcine monocyte population: A simple and efficient method. *Vet. Res. Commun.* **2013**, *37*, 239–241. [CrossRef]
46. Zhou, D.; Petersen, A.; Adelöf, J.; Hernebring, M.; Zetterberg, M. A Novel Primary Porcine Retinal Pigment Epithelium Cell Model with Preserved Properties. *Curr. Eye Res.* **2024**, *49*, 97–107. [CrossRef]
47. Wen, F.; Wang, Y.; He, D.; Liao, C.; Ouyang, W.; Liu, Z.; Li, W.; Liao, Y. Primary Culture of Porcine Retinal Pigment Epithelial Cells. *J. Vis. Exp. JoVE* **2022**, *187*, e64244. [CrossRef]
48. Toops, K.A.; Tan, L.X.; Lakkaraju, A. A detailed three-step protocol for live imaging of intracellular traffic in polarized primary porcine RPE monolayers. *Exp. Eye Res.* **2014**, *124*, 74–85. [CrossRef]
49. Hood, E.M.S.; Curcio, C.A.; Lipinski, D. Isolation, culture, and cryosectioning of primary porcine retinal pigment epithelium on transwell cell culture inserts. *Star Protoc.* **2022**, *3*, 101758. [CrossRef]
50. Wiencke, A.K.; Kiilgaard, J.F.; Nicolini, J.; Bundgaard, M.; Röpke, C.; La Cour, M. Growth of cultured porcine retinal pigment epithelial cells. *Acta Ophthalmol. Scand.* **2003**, *81*, 170–176. [CrossRef]
51. Lee, S.C.; Kwon, O.W.; Seong, G.J.; Kim, S.H.; Ahn, J.E.; Kay, E.D. Epitheliomesenchymal transdifferentiation of cultured RPE cells. *Ophthalmic Res.* **2001**, *33*, 80–86. [CrossRef]
52. Grisanti, S.; Guidry, C. Transdifferentiation of retinal pigment epithelial cells from epithelial to mesenchymal phenotype. *Investig. Ophthalmol. Vis. Sci.* **1995**, *36*, 391–405.
53. Dithmer, M.; Fuchs, S.; Shi, Y.; Schmidt, H.; Richert, E.; Roider, J.; Klettner, A. Fucoidan reduces secretion and expression of vascular endothelial growth factor in the retinal pigment epithelium and reduces angiogenesis in vitro. *PLoS ONE* **2014**, *9*, e89150. [CrossRef]
54. Williams, D.F.; Burke, J.M. Modulation of growth in retina-derived cells by extracellular matrices. *Investig. Ophthalmol. Vis. Sci.* **1990**, *31*, 1717–1723.
55. Huang, W.; Wang, L.; Yuan, M.; Ma, J.; Hui, Y. Adrenomedullin affects two signal transduction pathways and the migration in retinal pigment epithelial cells. *Investig. Ophthalmol. Vis. Sci.* **2004**, *45*, 1507–1513. [CrossRef]
56. Dörschmann, P.; Böser, S.; Isik, D.; Arndt, C.; Roider, J.; Selhuber-Unkel, C.; Klettner, A. Influence of carrier materials and coatings on retinal pigment epithelium cultivation and functions. *Exp. Eye Res.* **2022**, *219*, 109063. [CrossRef]
57. Wang, H.; van Patten, Y.; Sugino, I.K.; Zarbin, M.A. Migration and proliferation of retinal pigment epithelium on extracellular matrix ligands. *J. Rehabil. Res. Dev.* **2006**, *43*, 713–722. [CrossRef]
58. Viheriälä, T.; Sorvari, J.; Ihalainen, T.O.; Mörö, A.; Grönroos, P.; Schlie-Wolter, S.; Chichkov, B.; Skottman, H.; Nymark, S.; Ilmarinen, T. Culture surface protein coatings affect the barrier properties and calcium signalling of hESC-RPE. *Sci. Rep.* **2021**, *11*, 933. [CrossRef]

59. Park, J.H.; Jo, S.B.; Lee, J.-H.; Lee, H.-H.; Knowles, J.C.; Kim, H.-W. Materials and extracellular matrix rigidity highlighted in tissue damages and diseases: Implication for biomaterials design and therapeutic targets. *Bioact. Mater.* **2023**, *20*, 381–403. [CrossRef]
60. Wolfram, L.; Gimpel, C.; Schwämmle, M.; Clark, S.J.; Böhringer, D.; Schlunck, G. The impact of substrate stiffness on morphological, transcriptional and functional aspects in RPE. *Sci. Rep.* **2024**, *14*, 7488. [CrossRef]
61. Zhang, W.; Han, H. Targeting matrix stiffness-induced activation of retinal pigment epithelial cells through the RhoA/YAP pathway ameliorates proliferative vitreoretinopathy. *Exp. Eye Res.* **2021**, *209*, 108677. [CrossRef]
62. Husain, A.; Khadka, A.; Ehrlicher, A.; Saint-Geniez, M.; Krishnan, R. Substrate stiffening promotes VEGF-A functions via the PI3K/Akt/mTOR pathway. *Biochem. Biophys. Res. Commun.* **2022**, *586*, 27–33. [CrossRef]
63. Wendland, R.J.; Tucker, B.A.; Worthington, K.S. Influence of Substrate Stiffness on iPSC-Derived Retinal Pigmented Epithelial Cells. *Stem Cells Transl. Med.* **2024**, *13*, 582–592. [CrossRef] [PubMed]
64. Shi, H.; Sheng, G. The Adhesion and Neurite Outgrowth of Neurons on Poly(D-lysine)/Hyaluronan Multilayer Films. *J. Nanosci. Nanotechnol.* **2016**, *16*, 5506–5512. [CrossRef] [PubMed]
65. Kim, Y.H.; Baek, N.S.; Han, Y.H.; Chung, M.-A.; Jung, S.-D. Enhancement of neuronal cell adhesion by covalent binding of poly-D-lysine. *J. Neurosci. Methods* **2011**, *202*, 38–44. [CrossRef] [PubMed]
66. Stil, A.; Liberelle, B.; Guadarrama Bello, D.; Lacomme, L.; Arpin, L.; Parent, P.; Nanci, A.; Dumont, É.C.; Ould-Bachir, T.; Vanni, M.P.; et al. A simple method for poly-D-lysine coating to enhance adhesion and maturation of primary cortical neuron cultures in vitro. *Front. Cell. Neurosci.* **2023**, *17*, 1212097. [CrossRef]
67. Chang, C.W.; Ye, L.; Defoe, D.M.; Caldwell, R.B. Serum inhibits tight junction formation in cultured pigment epithelial cells. *Investig. Ophthalmol. Vis. Sci.* **1997**, *38*, 1082–1093.
68. Zhu, M.; Provis, J.M.; Penfold, P.L. Isolation, culture and characteristics of human foetal and adult retinal pigment epithelium. *Aust. New Zealand J. Ophthalmol.* **1998**, *26* Suppl. S1, S50–S52. [CrossRef]
69. Shen, H.; Wang, M.; Li, D.; Yuan, S.-T.; Liu, Q.-H. A novel xeno-free culture system for human retinal pigment epithelium cells. *Int. J. Ophthalmol.* **2019**, *12*, 563–570.
70. Kamei, M.; Lewis, J.M.; Hayashi, A.; Sakagami, K.; Ohji, M.; Tano, Y. A new wound healing model of retinal pigment epithelial cells in sheet culture. *Curr. Eye Res.* **1996**, *15*, 714–718.
71. Osusky, R.; Ryan, S.J. Retinal pigment epithelial cell proliferation: Potentiation by monocytes and serum. *Graefe's Arch. Clin. Exp. Ophthalmol.* **1996**, *234* Suppl. S1, S76–S82. [CrossRef]
72. Bhatia, S.K.; Rashid, A.; Chrenek, M.A.; Zhang, Q.; Bruce, B.B.; Klein, M.; Boatright, J.H.; Jiang, Y.; Grossniklaus, H.E.; Nickerson, J.M. Analysis of RPE morphometry in human eyes. *Mol. Vis.* **2016**, *22*, 898–916.
73. Ortolan, D.; Sharma, R.; Volkov, A.; Maminishkis, A.; Hotaling, N.A.; Huryn, L.A.; Cukras, C.; Di Marco, S.; Bisti, S.; Bharti, K. Single-cell-resolution map of human retinal pigment epithelium helps discover subpopulations with differential disease sensitivity. *Proc. Natl. Acad. Sci. USA* **2022**, *119*, e2117553119. [CrossRef] [PubMed]